# *The nocturnal water cycle in an open-canopy forest*




| | |
|---|---|
| **Citation** | Berkelhammer, M., J. Hu, A. Bailey, D. C. Noone, C. J. Still, H. Barnard, D. Gochis, G. S. Hsiao, T. Rahn, and A. Turnipseed (2013), The nocturnal water cycle in an open-canopy forest, Journal of Geophysical Research: Atmospheres, 118, 10,225-10,242. doi:10.1002/jgrd.50701 |
| **DOI** | 10.1002/jgrd.50701 |
| **Publisher** | American Geophysical Union |
| **Version** | Version of Record |
| **Citable Link** | http://hdl.handle.net/1957/47919 |
| **Terms of Use** | http://cdss.library.oregonstate.edu/sa-termsofuse |

# The nocturnal water cycle in an open-canopy forest

M. Berkelhammer,[1] J. Hu,[2] A. Bailey,[1] D. C. Noone,[1] C. J. Still,[3] H. Barnard,[4]
D. Gochis,[5] G. S. Hsiao,[6] T. Rahn,[7] and A. Turnipseed[8]

Received 22 December 2012; revised 31 July 2013; accepted 1 August 2013; published 12 September 2013.

[1] The movement of moisture into, out-of, and within forest ecosystems is modulated by feedbacks that stem from processes which couple plants, soil, and the atmosphere. While an understanding of these processes has been gleaned from Eddy Covariance techniques, the reliability of the method suffers at night because of weak turbulence. During the summer of 2011, continuous profiles of the isotopic composition (i.e., $\delta^{18}$O and $\delta$D) of water vapor and periodic measurements of soil, leaf, and precipitation pools were measured in an open-canopy ponderosa pine forest in central Colorado to study within-canopy nocturnal water cycling. The isotopic composition of the nocturnal water vapor varies significantly based on the relative contributions of the three major hydrological processes acting on the forest: dewfall, exchange of moisture between leaf waters and canopy vapor, and periodic mixing between the canopy and background air. Dewfall proved to be surprisingly common (∼30% of the nights) and detectable on both the surface and within the canopy through the isotopic measurements. While surface dew could be observed using leaf wetness and soil moisture sensors, dew in the foliage was only measurable through isotopic analysis of the vapor and often occurred even when no dew accumulated on the surface. Nocturnal moisture cycling plays a critical role in water availability in forest ecosystems through foliar absorption and transpiration, and assessing these dynamics, as done here, is necessary for fully characterizing the hydrological controls on terrestrial productivity.

**Citation:** Berkelhammer, M., J. Hu, A. Bailey, D. C. Noone, C. J. Still, H. Barnard, D. Gochis, G. S. Hsiao, T. Rahn, and A. Turnipseed (2013), The nocturnal water cycle in an open-canopy forest, *J. Geophys. Res. Atmos.*, *118*, 10,225–10,242, doi:10.1002/jgrd.50701.

## 1. Introduction

[2] Studies on the water budget of forests aimed at partitioning water fluxes and storage patterns [e.g., *Stewart and Thom*, 1973; *Calder*, 1998; *Anthoni et al.*, 2002] are needed to constrain the capacity of forests to respond to hydrological stress under different climate regimes [*Adams et al.*, 2009]. The response of forest ecosystems to hydrological change in turn has direct effects on regional precipitation patterns and temperature through land-atmosphere feedbacks [*Bala et al.*, 2007; *Gross*, 1987; *Spracklen et al.*, 2012] and also influences the global carbon budget through the dominant role that vegetation plays as a carbon sink [*Beer et al.*, 2010; *Luyssaert et al.*, 2007; *Myneni et al.*, 2001; *Keeling*, 1960]. The climate feedbacks between the land surface and atmosphere vary significantly between land surface models [*Lawrence and Chase*, 2009; *Pitman et al.*, 2009], indicating a need for continued efforts to develop more diverse observational constraints that can be used for model validation and development [*Still et al.*, 2009]. The eddy covariance technique (EC), which utilizes measurements of synchronous high speed wind and tracer concentration, has emerged as an essential approach to measure terrestrial ecosystem water and carbon fluxes [*Beer et al.*, 2010; *Baldocchi et al.*, 2001; *Massman and Lee*, 2002]. However, there remain some weaknesses in the EC approach associated primarily with the requirement for high levels of turbulence.

[3] During the development of the stable nocturnal boundary layer, lateral advection becomes an increasingly dominant flux term relative to turbulence [*Stull*, 1988],

Additional supporting information may be found in the online version of this article.

[1]Department of Atmospheric and Oceanic Sciences and Cooperative Institute for Research in Environmental Sciences, University of Colorado Boulder, Boulder, Colorado, USA.
[2]Department of Ecology, Montana State University, Bozeman, MT 59717.
[3]Forest Ecosystems and Society, Oregon State University, Corvallis, Oregon, USA.
[4]Department of Geography, Institute for Arctic and Alpine Research, University of Colorado Boulder, Boulder, Colorado, USA.
[5]Research Applications Laboratory, National Center for Atmospheric Research, Boulder, Colorado, USA.
[6]Picarro Inc., Santa Clara, California, USA.
[7]Earth and Environmental Sciences Division, Los Alamos National Laboratory, Los Alamos, New Mexico, USA.
[8]Atmospheric Chemistry Division, National Center for Atmospheric Research, Boulder, Colorado, USA.

Corresponding author: M. Berkelhammer, Cooperative Institute for Research in Environmental Sciences, University of Colorado Boulder, UCB 216, Boulder, CO 80309, USA. (max.berkelhammer@colorado.edu)


2169-897X/13/10.1002/jgrd.50701

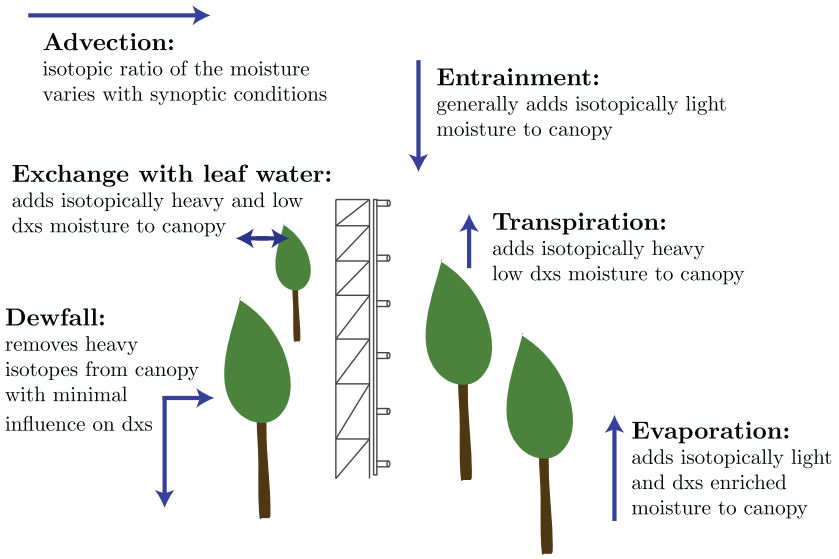


**Figure 1.** Schematic representation of the major processes discussed through the text and the isotopic change associated with this process.

which often negates the validity of the EC technique during the night. A number of studies have noted this issue and attempted to address it, for example, by applying filters of friction velocity and then interpolating across periods of low turbulence [*Loescher et al.*, 2006, and references therein]. Despite these efforts, collective knowledge of the nighttime water cycle in many ecosystems is limited. Nocturnal water fluxes may have a significant impact on water availability in some ecosystem and therefore observational constraints on these processes would improve understanding of water-ecosystem linkages. For example, water loss from the forest at night through transpiration may be of significant detriment to plant function in water-limited environments and the addition of ecosystem-available water through vertical movement of soil water [*Caldwell et al.*, 1998], and uptake of dewfall or fog condensation [*Dawson*, 1998; *Williams et al.*, 2008; *Stone*, 1963, *Malek et al.*, 1999] may be critical water sources for some plants and soil microbes [*Carbone et al.*, 2012].

[4] The ability to make in situ high-frequency (0.1–1 Hz) isotopic measurements of water vapor using laser absorption spectrometry [*Gupta et al.*, 2009; *Lis et al.*, 2008; *Tremoy et al.*, 2011] has emerged as a tool to complement EC techniques [*Welp et al.*, 2012; *Wen et al.*, 2008; *Lee et al.*, 2009; *Griffis et al.*, 2010]. The theory underlying the use of water isotope ratios to partition moisture fluxes is that isotopologues become fractionated during phase changes such that the heavier water preferentially remains in the liquid state. Diffusion of vapor imposes an additional fractionation as $H_2O$ can diffuse more quickly through air than deuterated water, which can diffuse more quickly than $H_2^{18}O$ [*Craig and Gordon*, 1965]. The former (i.e., phase change) is a thermodynamic process where the degree of fractionation (i.e., $\alpha$) is temperature dependent and has been well characterized for decades [*Horita and Wesolowski*, 1994]. The degree to which diffusional separation is expressed in water isotope ratios is largely dependent on the turbulent transport within the system [*Merlivat and Jouzel*, 1979].

[5] When considered in a global context, water isotope ratios (reported hereafter as $\delta^{18}O$ and $\delta D$ in ‰ units) form along a well-defined line with a slope near 8 and an intercept of 10 (i.e., the "global meteoric water line") [*Dansgaard*, 1964; *Merlivat and Jouzel*, 1979]. The slope arises as a product of the ratio of thermodynamic fractionation factors between hydrogen and oxygen while the intercept indicates the weighted-mean kinetic fractionation associated with the mean evaporative conditions (a function of humidity, turbulence, and temperature) over the ocean. Water samples that deviate from this line have been affected by additional kinetic processes (e.g., addition of moisture from continental evaporation or condensation under supersaturation) that are not characteristic of the conditions of open ocean evaporation. The magnitude of these kinetic effects are quantified using the second-order parameter, "deuterium excess" (dxs = $\delta D - 8*\delta^{18}O$), that is defined as the deviation of a sample (liquid or vapor) from the global meteoric water line.

[6] Decades of studies on isotopic pools in ecosystems provide the theory to understand how pools of water in a forest become isotopically distinct [*Brooks et al.*, 2010; *Flanagan et al.*, 1992; *Dawson and Ehleringer*, 1991; *Wang et al.*, 2010; *Yakir and Sternberg*, 2000; *Helliker et al.*, 2002; *Lai et al.*, 2006; *Lai and Ehleringer*, 2011; *Yepez et al.*, 2003; *Williams et al.*, 2004] (Figure 1). Evaporation of water from the soil surface yields a flux that is depleted in heavy isotopes and can be estimated knowing the isotopic ratio in the soil source water, surface humidity, temperature, and wind speed [*Allison and Barnes*, 1983; *Zimmermann et al.*, 1967]. Transpiration of moisture from plants at steady state (i.e., where the isotopic composition of moisture entering the leaf is equivalent to that leaving the leaf) is equal to the isotopic composition of the soil moisture weighted by the depth distribution of roots actively taking up soil water [*Yepez et al.*, 2003; *Wang et al.*, 2010]. However, because of trunk capacitance, there can be a lag between water that is actively being transpired and that which is taken in through

the roots [*Meinzer et al.*, 2005]. Differences in rooting distributions can produce variations in the transpiration flux between plant types that will depend on the vertical isotopic gradient in the soil water. The residual pools of water in both the leaves and surface soils tend to become enriched in heavy isotopes and have low dxs values, as a consequence of the strong kinetic fractionation associated with evaporation [*Allison et al.*, 1985]. As much as 10% of the water entering the leaves recirculates into the stem, resulting in stem water falling somewhere between soil and leaf water values. Additionally, because the isotopic ratio of water vapor in the troposphere decreases with altitude (following the decrease in water vapor mixing ratios with height), entrainment of air into the canopy from above will lead to moisture that is relatively depleted in the heavy isotope [*Lai et al.*, 2006; *Welp et al.*, 2012]. Condensation of water during dewfall or frost will selectively remove heavy isotopes from air through a largely equilibrium process [*Wen et al.*, 2012; *Noone et al.*, 2013]. Lastly, the isotopic composition of the vapor is significantly influenced by the degree of turbulence that affects both the boundary condition at the leaf and soil surfaces (i.e., the kinetic effects) and the amount of mixing that occurs between the canopy air space and open atmosphere [*Lee et al*., 2011].

[7] Here we report on high-resolution in situ isotopic measurements made from an open-canopy forest throughout an entire growing season. We focus on characteristics of the nighttime water cycle which, as discussed above, are difficult to delineate with EC measurements due to low nighttime turbulence. The measurements reported here emphasize and characterize the isotopic signature of a number of known processes, such as cold air drainage [*Vickers et al.*, 2012; *Blumen*, 1984; *Stull*, 1988], dew fall [*Wen et al.*, 2012; *Welp et al.*, 2012; *Jacobs et al.*, 2006; *de Roode et al.*, 2010], and exchange between canopy air and leaf/soil water pools [*Lai and Ehleringer*, 2011]. Using these measurements, we evaluate the importance that dewfall and water exchange across the stomata have on the nocturnal water cycle. The results suggest that a significant flux of moisture and latent heat is associated with dewfall and because some of the condensed water is likely sequestered through the leaf [*Kim and Lee*, 2011; *Boucher et al.*, 1995; *Munné-Bosch et al.*, 1999] and on the soil surfaces, it is a process that may significantly influence ecosystem productivity. We also find that the isotopic composition of vapor is strongly influenced by exchange across stomata, which can be used to track nighttime stomatal conductance and trace canopy vapor as it is flushed from the canopy in the morning by turbulence.

## 2. Methods

### 2.1. Site Description

[8] The Manitou Experimental Forest (MEF) is a mature open-canopy (LAI=1.9) ponderosa pine (*Pinus ponderosa*) forest in central Colorado (36°6'0"N, 105°5'30"W) [*DiGangi et al.*, 2011]. The site is located 45 km northwest of Colorado Springs, Colorado, and covers ∼67 km$^2$ in the South Platte River drainage. Elevation on the site ranges from 2300 to 2800 m. The site was heavily logged prior to its protection in 1936, and the mature trees range from ∼70 to 80 years old. The canopy height is between 12 and 20 m (average 18.5 m) and there is a low density understory of forbs, grasses, and pine saplings. The site has been utilized for experimental research since the late 1930s [*Johnson*, 1956; *Schuster*, 1964], with early studies focusing on the impact of grazing on ecosystem diversity and health. More recently, the forest has been the home for a number of intensive studies on biosphere-atmosphere-climate feedbacks [e.g., *DiGangi et al.*, 2011, 2012; *Kim et al.*, 2010; *Kaser*, 2013] and for experimental studies on fire impacts [*Massman et al.*, 2008]. These recent studies facilitated the installation and upkeep of a number of flux towers on the site (described in sections 2.2 and 2.4), which were utilized extensively in this study. During the growing season, short-lived convection produces sporadic precipitation while additional precipitation occurs as snowfall during the winter months [*Schuster*, 1964]. There is an intermittent snow pack lasting until early spring when the snowmelt pulse can saturate the soil for days to weeks depending on weather conditions (supporting information Figure 2). For more detailed descriptions of the site climatology, the reader is referred to the following texts: *DiGangi et al.* [2011, 2012], *Kim et al.* [2010], and *Kaser* [2013].

### 2.2. Vapor Analysis

[9] In May of 2011, a Picarro L2120-i isotopic analyzer was installed in a temperature-controlled trailer at the base of a 27.1 m tower situated amid a stand of ponderosa pines in the MEF. The flux footprint for the tower is estimated to be ≤ 900 m during unstable conditions and ≤2500 m for stable conditions [*Kaser*, 2013]. Within this footprint, the stand is essentially homogeneous (i.e., low density, mature *Pinus ponderosa*). The isotopic analyzer sampled water vapor from six 1/4" teflon lines that were insulated and lightly heated with self-regulating heat trace just above ambient temperatures. The inlets were positioned at approximately 1.5, 5.0, 8.5, 12.0, 17.7, and 25.1 m on the tower. The inlet lines were all of equal length (to yield similar lag times) and were pumped at a rate of approximately 3.5 standard liters per minute producing an 8–12 s lag between the inlet and analyzer. Upon entering the trailer, the six lines were plumbed into a solenoid manifold, which pulled air from each height for 5 min before switching to the adjacent sampling line (supporting information Figure 1). In this configuration, a complete vertical profile was measured every 30 min producing 48 complete profiles each day. Further descriptions of the system can be found in *DiGangi et al.* [2011].

[10] The raw isotopic measurements were processed by initially removing the first 3 min after each valve switch to accommodate the memory associated with the tube connecting the valve manifold and the instrument's optical sample cavity. The filtering time was chosen to conservatively remove the effects of memory, while still providing sufficient time to establish a stable baseline measurement before switching heights. The remaining 2 min of data was averaged together to produce approximately 48 measurements from each height every day. The average isotopic measurements were calibrated with reference to the international standard Vienna Standard Mean Ocean Water (VSMOW) by introducing a pair of standard waters approximately every 6 h that span the range of isotopic values observed in the field. The introduction of standards was done using the commercially available Standards Delivery Module from Picarro Inc. In this system, two standard waters are stored in sealed

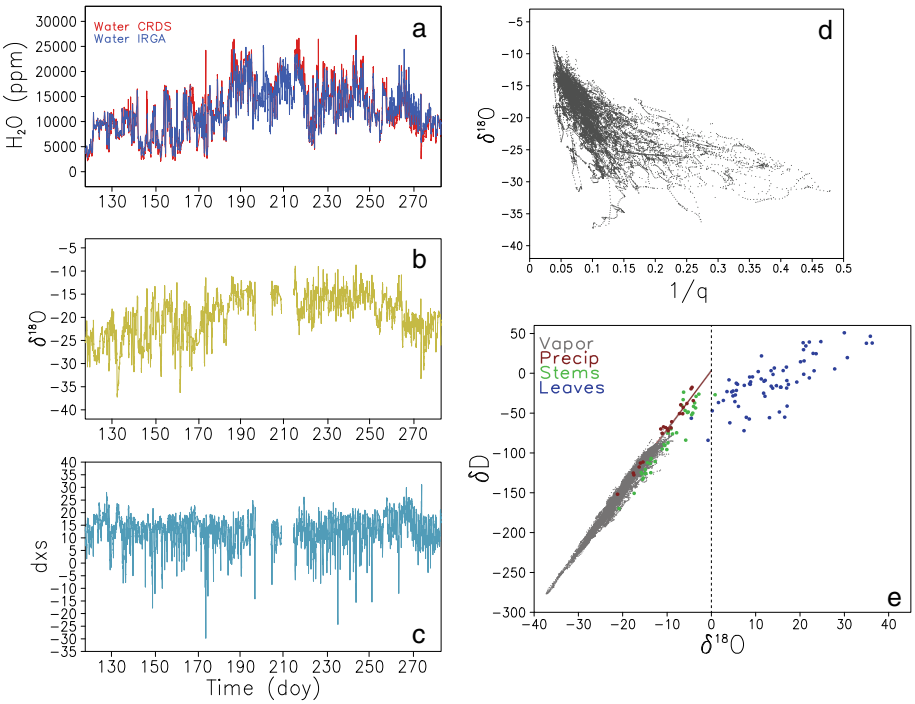


**Figure 2.** (a) Time series showing the measured specific humidity at the 17.1 m level and the corresponding humidity measured using an Infrared Gas Analyzer (IRGA) on the tower at the same height as the inlet line. (b) Time series showing the $\delta^{18}O$ at the 17.1 m height during the course of the sampling campaign. (c) Time series showing the deuterium excess at the 17.1 m height during the course of the sampling campaign. (d) The relationship between specific humidity and $\delta^{18}O$ and (e) the meteoric water line for vapor, liquid, precipitation, stem, and leaves. The red and gray lines indicate the Local Meteoric Water Line for precipitation and vapor samples, respectively.

bags and introduced by a syringe into a vaporizer system kept at 140°C using a continuous stream. The velocity of the water stream is controlled by a high precision syringe pump. The standard water vapor is mixed with a dry air stream (created by pulling dry air through a desiccant) to produce air with different humidities but the same isotopic values. The calibration stream is introduced into the isotopic analyzer through a three-way solenoid valve that switches between air samples from the tower and from the two standard vapors. Standards were typically introduced for periods of 10–20 min to produce a single well-constrained mean isotopic measurement. The setup is comparable in form to the calibration system and sampling strategy of *Tremoy et al.* [2011] and is shown schematically in supporting information Figure 1.

[11] Because of difficulties in producing accurate low humidity calibration points with the field calibration system, a series of "humidity calibrations" were performed in the laboratory prior to and following the campaign. It is known that isotopic analysis using Cavity Ringdown Spectrometry (CRDS) instruments is sensitive to humidity [*Tremoy et al.*, 2011], an effect that is both instrument specific and can be very severe at low humidities. Characterization of the humidity dependence of this instrument was done using a "saturation bubbler", where ultra-dry air is bubbled through a fritted tube plumbed into a leak-tight temperature-controlled 5 L basin of water [*Steen-Larsen et al.*, 2013]. The temperature of the water source is maintained by placing the bubbler system inside a freezer that is filled with water to provide a medium with high thermal inertia. The temperature of the system is controlled by a proportional integral derivative controller that sends power to the condenser or heating coil in order to maintain stable temperatures of ±0.1°C. The flow of dry air is controlled using a mass flow controller, and the saturated air that bubbles out of the water bath is mixed with dry air (supporting information Figure 1). The humidity of the vapor can be controlled both by changing the dilution of the saturated flow or the flow rate through the bubbler system. The moist air is introduced into the isotopic analyzer through an 1/8" copper tube, and an open split is maintained just upstream from the instrument to allow the system to vent continuously. The humidity dependence was tested pre- and post-deployment across the span of humidity values measured in the field (4000–30,000 ppm). A curve was then fit to the humidity and isotopic data, and the uncertainty was evaluated as the difference between the humidity-dependence curves before and after instrument deployment.

[12] All data were processed in the following order: (1) the last 2 min of data following every solenoid switch was averaged, (2) these values were then corrected for their humidity dependence using the average of the pre- and post-deployment curves, (3) all isotopic values were corrected to the absolute VSMOW scale and instrument drift was removed by fitting a curve between measured and known values for the water standards, and (4) values were linearly interpolated onto a 30 min evenly spaced timescale to allow for synchronous vertical profile information. There was no

evidence for diel cyclicity in the standards, so there was no need to apply any further correction based on temperature variations in the instrument trailer. No time-dependent correction to the absolute humidity was applied because the measured humidity values from the isotopic analyzer and the humidity values measured with a closed-path Infrared Gas Analyzer (IRGA) system (described below) located at the 25.1 m inlet tracked each other closely ($r^2 = 0.92$), though a uniform correction was applied to account for a high humidity bias of 4%–6% for the Picarro (Figure 1).

[13] The uncertainty in the reported isotopic values arises from three processes (in descending order of importance): (1) the absolute isotope correction (i.e., standardization to VSMOW), (2) the standard deviation of the 2 min average, and (3) the humidity dependence (which turns out to be negligible at humidities greater than 5000 ppmv). Because data hereafter are reduced to a series of diel composites, uncertainty is reported as standard error, defined as $\frac{S}{\sqrt{n}}$, where $S$ is the standard deviation of the sample mean and $n$ is the size of the composite (i.e., number of measurements). Composites were calculated as the unweighted mean of 30 min resolved 24 h cycles. Composite analysis allows the uncertainty to be greatly reduced because the variance on the mean of the distribution of all observations in each composite is far smaller than the variance in the raw data.

### 2.3. Liquid Analysis

[14] Through the course of the experiment, numerous isotopic measurements were made on leaf, soil, stem, and dew waters. Precipitation was collected following every storm of the season ($n = 16$) using a simple funnel collector with a mineral oil layer used to prevent evaporation and subsequent isotopic fractionation [*Friedman et al.*, 1992], and grab samples of surface snow were taken in the early and later part of the campaign. Surface soil waters were cryogenically extracted on a high vacuum extraction line following *West et al.* [2006], and isotopic analysis was conducted using a Picarro L2120-i isotopic analyzer using a LEAP PAL (™) autosampler for injection and a Picarro vaporizer to convert the liquid to vapor (supporting information Figure 1). Unlike leaf and stem waters, which are known to contain organic materials that influence the credibility of the spectroscopy [*West et al.*, 2006; *Schultz et al.*, 2011; *Schmidt et al.*, 2012], soil waters at this site yielded low concentrations of organics and so could be analyzed without the need for spectral correction.

[15] Water was extracted from the leaf and stem materials through a novel induction heating process, which has the advantage (relative to the cryogenic water extraction approach) of increased throughput, a capacity to provide reliable measurements on very small samples, the use of pyrolysis to remove organic contamination, and the ability to measure samples directly in the field. The collected samples (debarked stems and pine needles) were wrapped in small metal sleeves (to facilitate the induction heating), placed inside 4 mL glass vials, and sealed with a septa-insert cap. The sample vial is inserted into the Induction Module (IM), and the septa is punctured by a double needle. Ambient air is pushed out of the vial by allowing pressurized dry air to flush through the vial and out the second hole in the double needle. The sample is then heated through induction by a user-specified ramp function to 100°–200°, depending on the sample (hotter for soils and stems than leaves). The resulting vapor is carried on a dry air stream through a ceramic micropyrolysis column that is maintained at approximately 1200°C, which breaks down the majority of compounds that are known to interfere with the spectroscopy [*West et al.*, 2010]. The resulting flow travels past an open split and directly into the isotopic analyzer (supporting information Figure 1). The water vapor stream is measured continuously, and a single isotopic value for the sample is found by integrating across a region where humidity exceeds a given threshold (in this case, 1000 ppmv). The system was operated in a rapid analysis mode with relatively short (5–10 min) extraction times. We recognize this approach would fail to extract some tightly bounded waters [*Brooks et al.*, 2010]. However, for the purposes of broadly characterizing the bulk water pools, our extraction efficiencies generally exceeded 95% of the total water (based on the measured decay of humidity coming off the material) and were therefore adequate for the purposes of this study. Dew water was also measured using this technique by running dried filter paper across a dew-soaked surface and taking a small piece of the saturated paper and introducing it into the induction heating system as described above. Throughout the course of the IM analysis, standards were run by placing a few microliters of standard water on small pieces of dried filter paper.

[16] The approach described here is experimental, and a number of significant issues became apparent during the processing of samples. Strong memory affects were detected, which reduced independence between adjacent samples. To address this, the first measurement of every sample was rejected and, in some cases, as many as the first 5–6 measurements of a given sample were discarded. The discarded samples were identified as those where the influence of the previous measurement was clearly distinguishable (i.e., repeat measurements still contained a trend). Despite repeat measurements on individual samples and the inclusion of blank analysis between samples, these effects could not be confidently removed. The memory effect was most severe in the oxygen isotopes, which is hypothesized to arise because of isotopic exchange between the sample vapor and the micropyrolysis column. Laboratory experiments show this behavior to be a function of column temperature, and values are consistent with known temperature effects on the isotope exchange between alumina and water. The root cause of the memory effects in deuterium are not well known though may relate to moisture adsorbing onto the interior surfaces of the valves and plumbing in the IM system. Because of the poor reproducibility arising from this issue, the distribution of leaf ($n = 71$), stem ($n = 41$), and dew ($n = 17$) waters was used to produce a likely range of values for each of these water pools. Despite the known issues with the approach, we have confidence in the general veracity of the method based on several lines of evidence. First, the isotopic enrichment along single leaves is consistent with values observed through cryogenic extraction and Isotope Ratio Mass Spectrometry (not shown) [*Farquhar and Gan*, 2003; *Shu et al.*, 2008], second, the slope of $\delta D$ versus $\delta^{18}O$ in the stem waters falls along the slope derived from precipitation samples (i.e., the local meteoric water line) measured (Figure 2), and third, the filter paper calibrations and blanks provided a sound reference.

### 2.4. Additional Measurements

[17] The experiment was conducted synchronously and in coordination with the BEACHON-RoMBAS experiment (https://nar.ucar.edu/2010/lar/page/beachon-0), and thus, many additional measurements were available from the site. A pair of Decagon Leaf Wetness Sensors (LWS) was located near the base of the tower approximately 10 cm from the surface of the ground. These instruments measure the presence of water on the surface of a dielectric sensor designed to mimic the surface of a leaf. Raw voltages from the Leaf Wetness Sensors were read by a Campbell Scientific Datalogger, and the data were analyzed as raw single-ended voltage measurements. Two profiles (5, 50, 70, 100, and 150 cm depths) of volumetric water content were measured using Decagon EC-5 dielectric probes. Soil moisture was measured in the canopy near the base of the tower where the isotopic measurements were made. Air temperature, relative humidity, and air pressure were measured from a series of Vaisala HMT337 and WXT520 probes located at 1, 7, 14, and 27 m on the tower. $H_2O$ and $CO_2$ fluxes were estimated using the eddy covariance method with high speed wind measurements from a Campbell CSAT-3 sonic anemometer (at 25.1 m) that was collocated with an inlet plumbed into a Licor Li-7000 infrared gas analyzer in the instrument shed. Details on the calculation of the fluxes can be found in *Kaser* [2013] and *DiGangi et al.* [2011]. Radiation (net, longwave, shortwave, and photosynthetically active) was measured using a Kipp and Zonen CNR1 4-channel radiometer at 25 m on a nearby tower (approximately 500 m away) in the footprint of the other tower. This second tower also included a LiCor Li7500 used for open-path $CO_2$ and $H_2O$ measurements. Six custom sap flow sensors were installed at ∼1.5 m heights in the trunks of mature average height *Pinus ponderosa* trees using the heat pulse method described by *Burgess et al.* [2001]. These sensors were installed on trees well within the footprint (900-2500m) of the tower used for the isotopic measurements. All data utilized in this study were calibrated as described by *Kaser* [2013] and *DiGangi et al.* [2012] and are publicly available from cires.colorado.edu/jimenez-group/wiki/index.php/BEACHON-RoMBAS. The data were binned onto a common 30 min timescale as done with the isotopic data.

### 2.5. Data Processing

#### 2.5.1. Clustering

[18] To characterize dominant nocturnal processes, a multivariate *k*-means clustering algorithm was employed on the 132 available diel cycles. In *k*-means clustering, the purpose is to take a series of "objects", in this case a diurnal cycle of a given field, and partition these objects into a fixed number of groups (clusters) in a way that minimizes the distance between the objects within a cluster and maximizes the distance between clusters. Within each cluster, a "centroid" is defined as the average value of all the objects in the group and "distance" is defined as the sum of the absolute difference between an object and the cluster centroid. In using *k*-means clustering, a set number of clusters must be defined a priori and a metric chosen to define distance between an object and the centroid. For example, distance could be calculated as the Pearson's correlation coefficient between object and the centroid or as the absolute differences between object and centroid.

[19] To solve for the best solution to the clustering algorithm (i.e., where the distance between objects within a cluster and the centroid is minimized and distance between centroids is maximized), an iterative approach must be used. Centroids for each of the fixed number of clusters are randomly chosen, and the solution is found that places each object into a cluster while minimizing the within-cluster distance. We then repeat this procedure by reinitializing the centroids 10,000 times, each time iteratively solving for the solution that minimizes distance. The final solution places each object into a cluster based on the frequency of an object being clustered together throughout the iterations. These calculations were done using the standard clustering package available with the MATLAB ® software (distance calculated using the *City Block* algorithm). Experiments were tried with different distance metrics and numbers of iterations and the solutions were similar. Ultimately, we found that four clusters were best for the multivariate clustering and that the fields used were specific humidity, deuterium excess (dxs = $\delta D - 8{*}\delta^{18}O$), and relative humidity time series data. Unless otherwise specified, all subsequent discussion focuses on the centroid (median) of each cluster with uncertainty represented as the standard error of the cluster. This approach to analyzing isotopic data allows for a delineation of first-order "types of days" and, unlike Principal Component Analysis, does not require any data normalization. A small number of cycles was removed because of either data gaps or the presence of sustained rainfall, which produced stochastic features biased by rapid cycling of liquid water on surfaces and the canopy air space and not representative of the exchanges associated with persistent processes.

#### 2.5.2. Flux Analysis

[20] As described previously by *Williams et al.* [2004], *Wang et al.* [2010], and *Noone et al.* [2013], the inverse gradient approach of *Keeling* [1958] can be employed to determine the isotopic composition of the water flux if the process(es) is occurring amidst an isotopically stable background. The original derivation of the inverse gradient approach shows that the intercept of the linear regression between $\frac{1}{[H_2O]}$ and $\delta$D or $\delta^{18}$O is equivalent to the isotopic composition of the flux. *Miller and Tans* [2003] show that the influence of type 2 regression errors can be minimized if the flux is treated as the slope of the following linear equation (where $q$ is water concentration), whose value converges on the original inverse gradient approach as the $r^2$ of the fit approaches 1 [*Pataki et al.*, 2003]:

$$q{*}\delta D = q{*}\delta D_{\text{flux}} - \left[q_{\text{background}}\left(\delta D_{\text{flux}} - \delta D_{\text{background}}\right)\right] \quad (1)$$

[21] The equation is applied here using the vertical gradient between inlets [*Still et al.*, 2003; *Griffis et al.*, 2007]. Because the land surface within the footprint is essentially homogenous for both stable and unstable conditions [*Kaser*, 2013], no discussion of changes in footprint size are considered when interpreting the flux data. We perform the gradient analysis separately for inlet lines near both the bottom of the canopy (1.5–12 m) and the upper part of the canopy (12–25.1 m) to distinguish processes that may be focused on the surface or in the foliated region in the upper canopy.

**Table 1.** Frequency and General Description of the 4 Dominant Clusters Discussed in the Text

| Cluster Name | Number of Days | $\delta$ Trend | dxs Trend | Humidity Trend | Process |
|---|---|---|---|---|---|
| Cluster 1 | 24 | Rise | Drop | Rise/Stable | Canopy Vapor-Liquid Exchange |
| Cluster 2 | 21 | Drop | Stable | Drop | Canopy-Wide Dewfall |
| Cluster 3 | 21 | Drop | Stable | Drop | Foliation Dewfall |
| Cluster 4 | 90 | Stable | Stable | Stable | Mixing With Above-Canopy Air |

[22] Estimates of the isotopic composition of the flux were done using a Mixed Effects Model (MEM) [*Nippert et al.*, 2010] to reduce the influences that processes (both random and fixed) have on the solution to equation (1). In most other discussion in the manuscript, we focus on the centroid of a given cluster, but for the MEM analysis, the regression model (equation (1)) is calculated at a given time step for each object within a cluster. For example, Cluster 1 contains 24 days (Table 1) and therefore 24 regression models describing the gradient are possible for each time step. MEM finds the solution to $\delta D_{\text{flux}}$ from equation (1) that minimizes bias in the residuals of the model by accounting for effects arising within this population of objects. Uncertainty in the flux estimates are reported as the mean squared error of the MEM model.

[23] In the theoretical case where the canopy air space is completely isolated from the atmosphere above, changes in the isotope ratios that accompany condensation can be captured using a Rayleigh distillation model, where moisture is instantaneously condensed out of the air column and fractionates according to the temperature and humidity of the surface where condensation is occurring. The Rayleigh distillation model is described using equation (2), where $f$ is the fraction of moisture remaining, $\delta^{18}O^o$ specifies the isotopic ratio of the initial moisture source, and $\alpha_{\text{eff}}$ is the fractionation factor, which is the product of equilibrium and kinetic effects. The equilibrium fractionation factor is calculated from the equation in *Majoube* [1971], and the kinetic fractionation factor is calculated using the technique in *Lee et al.* [2009]. The magnitude of kinetic fractionation varies with the total resistance of the canopy air space and approaches pure molecular diffusion [*Merlivat and Jouzel*, 1979] in a completely stable atmosphere.

$$\delta^{18}O = \delta^{18}O^o * f^{(\alpha_{\text{eff}}-1)} \tag{2}$$

[24] A box model is constructed assuming that dewfall is a Rayleigh distillation process (supporting information Figure 3). In the model, the canopy is treated as vertically stacked distillation columns with the bottom of the upper column ending at the height where the maximum

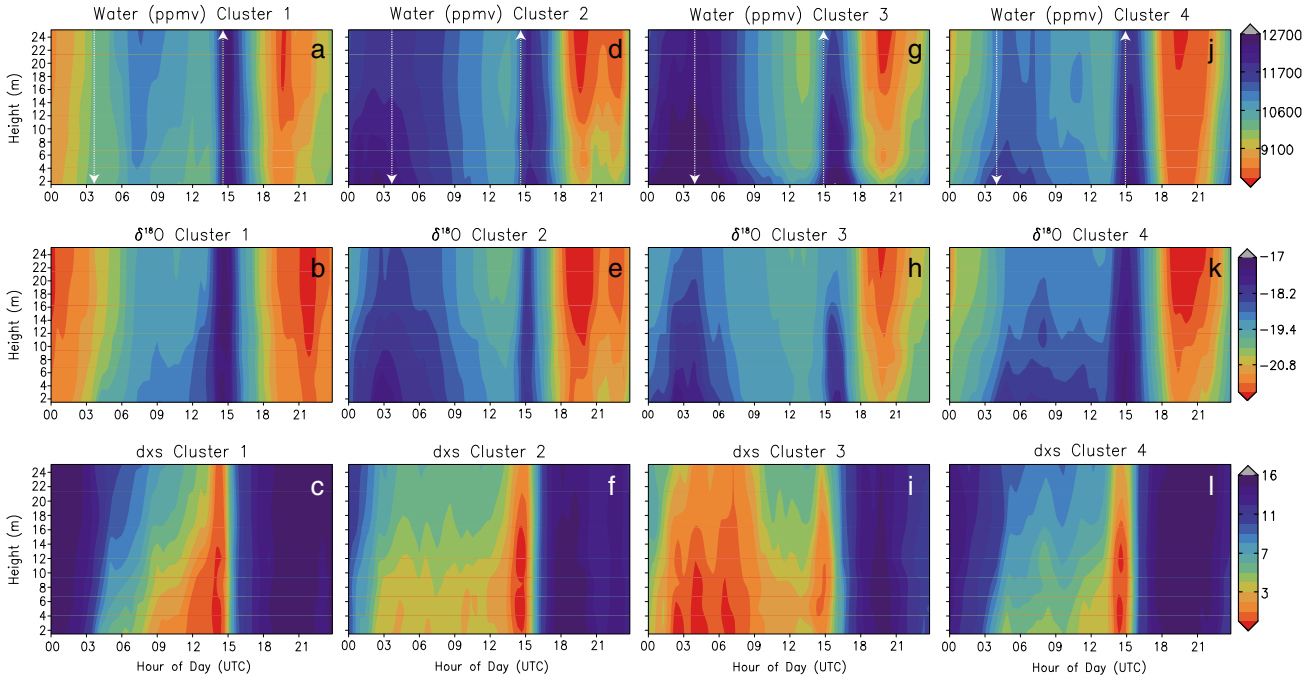


**Figure 3.** Vertical profiles of the diel cycle of specific humidity (a, d, g, and j), $\delta^{18}$O (b, e, h, and k), and deuterium excess (c, f, i, and l) for each of the four clusters. The panels correspond to a 24 h period on the universal time coordinated (UTC) time scale (i.e., local time shifted forward by 7 h). The approximate times of sunset and sunrise are marked by upward and downward arrows, respectively. Refer to Figure 8f to see downward shortwave radiation.

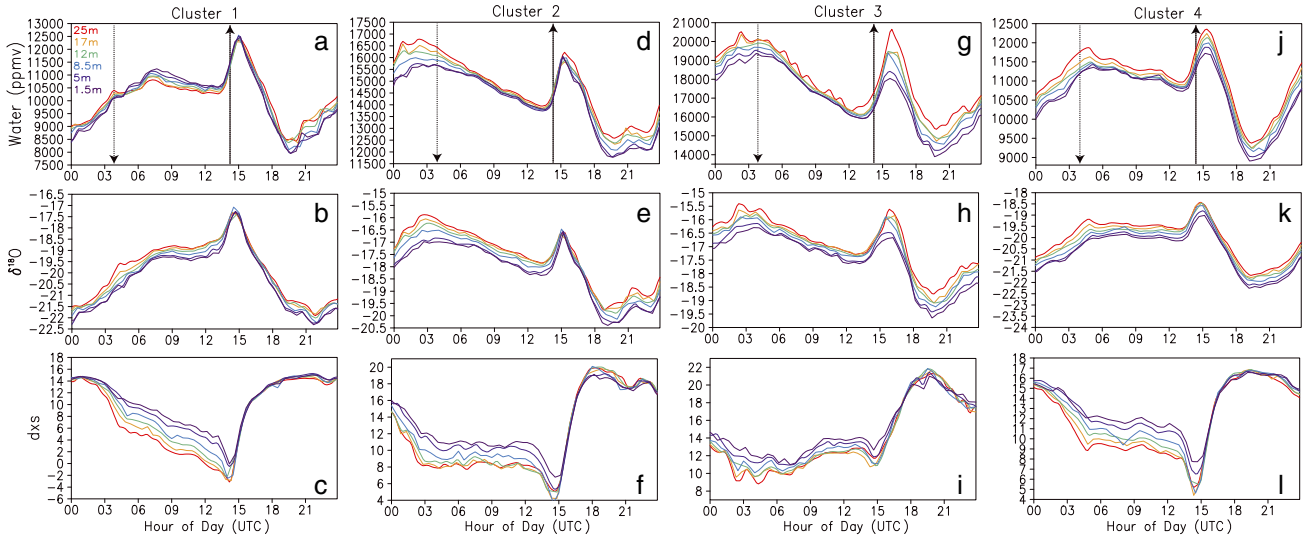


**Figure 4.** Time series for each of the different inlets of the diel cycle of specific humidity (a, d, g, and j), $\delta^{18}$O (b, e, h, and k), and deuterium excess (c, f, i, and l) for each of the four clusters. The panels correspond to a 24 h period on the UTC time scale (i.e., local time shifted forward by 7 h). The information is the same as in Figure 2 except for the data are presented as time series.

density of leaves is located (12 m) and the bottom of the second column at the ground. The isotopic value of the moisture in the column is estimated using equation (2), where $f$ is calculated as the fractional change in the water volume mixing ratio since the beginning of the night and $\alpha_{\text{eff}}$ is estimated using the method of *Lee et al.* [2009] where measured temperatures from the tower are used to estimate the fractionation factor during phase change. To account for transport from turbulence within the canopy, we assume each of the stacked distillation columns is separated into two separate boxes where the upper box does not experience any condensation. Rather, water is lost through downward transport into the lower box which is modeled using a diffusion equation. Here again, the isotopic ratio of the vapor is treated as a Rayleigh distillation process, except the $\alpha_{\text{eff}}$ term accounts for kinetic fractionation that arises from molecular diffusion during phase change out of equilibrium.

[25] An additional approach used here to estimate the isotopic composition of the dew flux is derived from the equation described in *Wen et al.* [2012] (equation (3)). This equation is based on a gradient approximation where $\epsilon=(\alpha-1)*1000$, $h$ is relative humidity, $\epsilon_{\text{equil}}$ is the temperature-dependent fractionation that accompanies a phase change, and $\epsilon_{\text{kinetic}}$ is the fractionation associated with diffusion. The equation is derived following the classic Craig-Gordon equation [*Craig and Gordon*, 1965] where total fractionation is the sum of the resistance of the different isotoplogues across a series of atmospheric layers, with the surface being saturated and the uppermost layer being characterized by ambient humidity.

$$\delta^{18}O_{\text{dew}} = \left( \frac{\delta^{18}O_{\text{vapor}} + \epsilon_{\text{equil}}/h + (1-h)*\epsilon_{\text{kinetic}}/h}{1 + \epsilon_{\text{kinetic}}/1000 - (1-h)*\left(\epsilon_{\text{equil}} + \epsilon_{\text{kinetic}}\right)/1000} \right) \quad (3)$$

## 3. Results

### 3.1. Seasonal Trends

[26] The isotopic composition of moisture at the MEF site is characterized by a strong seasonal cycle in both $\delta$D and $\delta^{18}$O (Figure 2b) that broadly follows the specific humidity (Figure 2c) along a reverse exponential fit (Figure 2d). Minimum values during the sampling campaign of –280.1‰ and –37.3‰ for $\delta$D and $\delta^{18}$O, respectively, were observed in mid-October and maximum values for $\delta$D and $\delta^{18}$O of –58.1‰ and –8.6‰ were recorded in early August (Figure 2b). The isotopic seasonal cycle is characterized by a slow rise from May to August followed by a fairly rapid decline to the fall minima.

[27] Isotopic measurements of precipitation largely follow the seasonal cycle in vapor with maxima for precipitation of –4.0‰ in $\delta^{18}$O (–17.6‰ for $\delta$D) in August and minima of –21.1‰ for $\delta^{18}$O (–151.7‰ for $\delta$D) in October (Figure 2e). Periodic measurements of stem waters from mature pines within the flux footprint throughout the season broadly follow the same cycle seen in the precipitation. The stem waters are offset positively from the precipitation reflecting some combination of the fact that soil waters are evaporatively enriched and also that water in the stem experiences some mixing with the isotopically enriched waters in the leaf. Unlike stem water, which track the soil water (i.e., the precipitation inputs), the leaf waters are significantly influenced by high-frequency changes in relative humidity and leaf temperature which influence the degree of evaporative enrichment affecting these smaller and more dynamic pools. Consequently, the seasonal cycle in leaf waters is less apparent.

[28] When plotted in the $\delta$D–$\delta^{18}$O space, the vapor measurements fall along the same line (within statistical uncertainty) as the precipitation samples though are offset negatively (in both $\delta$D and $\delta^{18}$O) with a magnitude

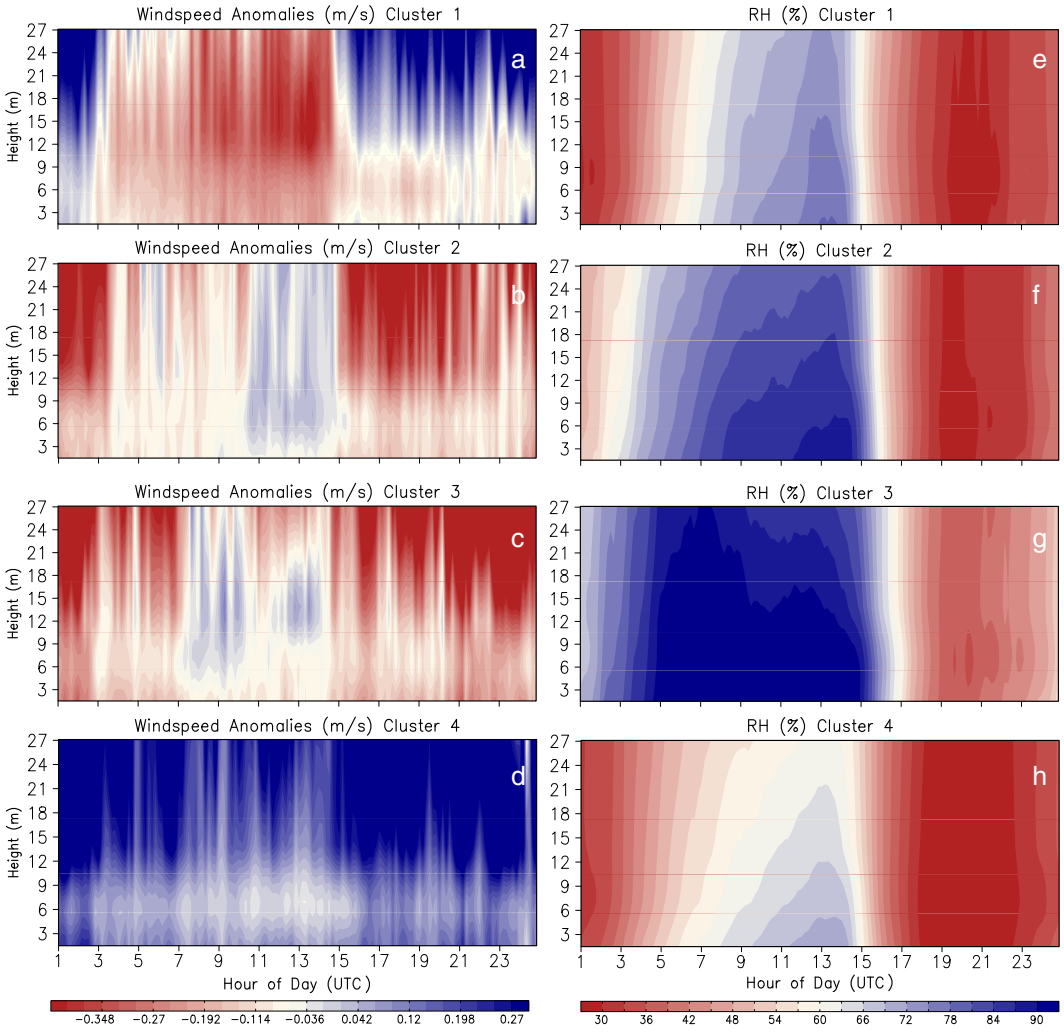


**Figure 5.** (a–d) Composite wind anomalies relative to the mean diel wind profile for Clusters 1–4 (shown in descending order). The profiles were generated using 30 min averaged wind speeds from four cup anemometers distributed vertically on the tower. (e–h) Composite diel cycles of the relative humidity profiles for the four clusters (shown in descending order).

that is consistent with the temperature dependence of the equilibrium fractionation factor between vapor and liquid (Figure 2e) [*Strong*, 2012]. The leaf waters fall significantly to the right of the vapor and other liquid samples, which is a product of the strong kinetic influences of evaporation.

[29] Deviations from the line defining the covariation of $\delta$D and $\delta^{18}$O are characterized using the deuterium excess (dxs) parameter. Unlike the first-order isotopic composition values, dxs in the precipitation, stem water, and vapor pools do not display a measurable seasonal cycle but show diel variability (in the vapor) that is more pronounced than either of the isotope species (Figure 2c). The stability of dxs values in the low frequency reflects a general consistency in the kinetic conditions in the moisture source regions despite changes in the large-scale atmospheric circulation regimes that characterize the seasons. The kinetic effects of evaporation, however, give rise to extremely negative dxs values in both the surface soil and leaf water pools with values in some instances reaching below –100‰ which is consistent with the values seen in leaf water samples in previous studies (e.g., *Allison et al.* [1985]). The kinetic effects of evaporation are seen, though more subdued, in the stem water pools, reflecting both the fact that the trees are drawing on some shallow soil waters that have experienced evaporation and that mixing between stem and leaf water pools occurs.

### 3.2. Cluster 1: Vapor-Liquid Exchange Within the Canopy

[30] Cluster 1 is associated with nights where the water vapor mixing ratio at all levels increases in the early evening but remains nearly stable until morning when there is a rapid increase in humidity (Figures 3a–3c and 4a–4c). During the period of stable canopy humidity, there is a slight, though persistent, rise in both $\delta$D and $\delta^{18}$O and a dramatic decline in dxs. This cluster is associated with wind speeds that are, on average, slower than the other clusters (Figure 5). The lack of strong winds or dewfall results in the presence of a strong isotopic signature of exchange between surface liquid pools (soil and leaf) and vapor.

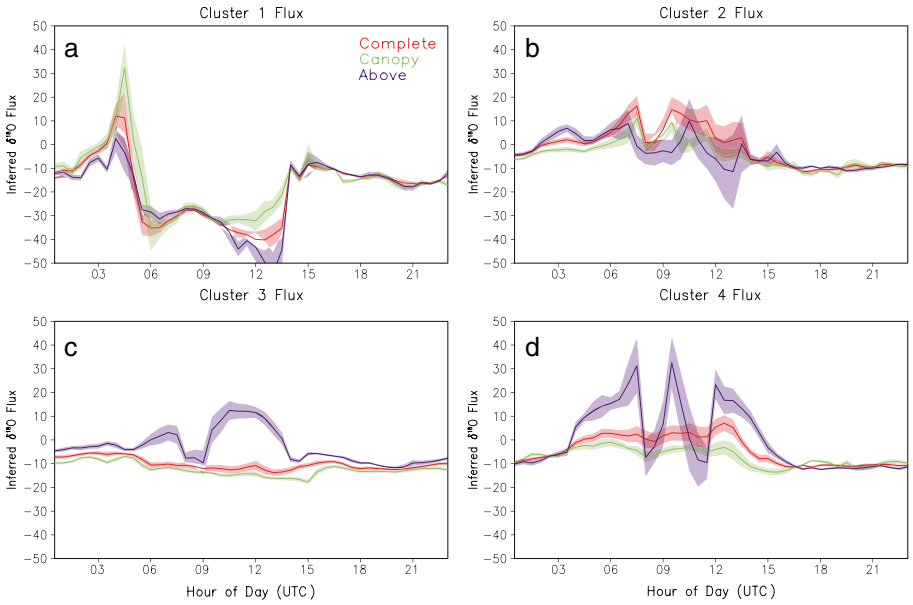


**Figure 6.** Mixing line estimates of the $\delta^{18}O$ of the flux that drives the isotopic changes for the four clusters. The flux estimate was calculated hourly using a mixed effects model for all six vertical points ("complete"), the lower four points ("canopy"), or the upper three points ("above"). The shading captures the mean squared error of the flux estimates based on the mixed effects model (equation (1)). While daytime fluxes are very consistent between the clusters, clear deviations emerge during the nights. Sunset is approximately equivalent to "Hour 3.3" and sunrise "Hour 14.5" (see arrows in Figure 2).

[31] Using a mixing line estimation of the isotopic composition of the water flux [*Miller and Tans*, 2003] (Figure 6a), Cluster 1 is found to be associated with a rapid transition between an isotopically enriched and depleted flux in the early and later parts of the evening, respectively. The transition in the fluxes occurs when skin and air temperatures become equivalent. The relaxation of the surface to air temperature difference diminishes the presence of a vapor pressure gradient between the surface and the canopy air and therefore total water flux from the surface to the canopy ceases (i.e., specific humidity does not continue to rise). The evenings in this cluster account for 12% of the measured nights and tend to occur in the early portion of the growing season prior to the onset of summer storms but when soil moisture at depth (40–70 cm) is still high from snowmelt (supporting information Figure 2).

### 3.3. Cluster 2: Dewfall Across the Canopy

[32] Cluster 2 accounts for 14% of the nights and occurred most commonly in the middle to later portions of the

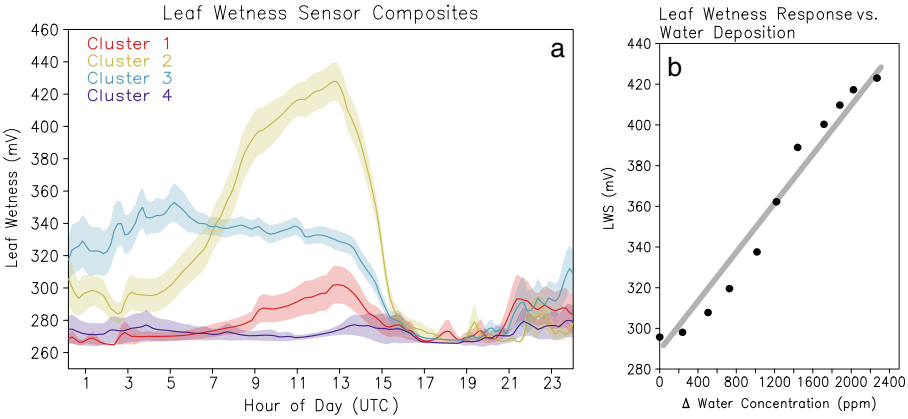


**Figure 7.** (a) Composite surface leaf wetness data for the four clusters where shading shows the standard error for the cluster. The units are raw mV coming off the dielectric sensor. (b) Moisture deposition as a function of leaf wetness (LWS). Water deposition ("$\Delta$ Water Concentration") is the absolute value of the change in water volume mixing ratio since the beginning of the dewfall period. "LWS" is the cluster-averaged leaf wetness over this period. The line is the result of a linear regression analysis between these variables.

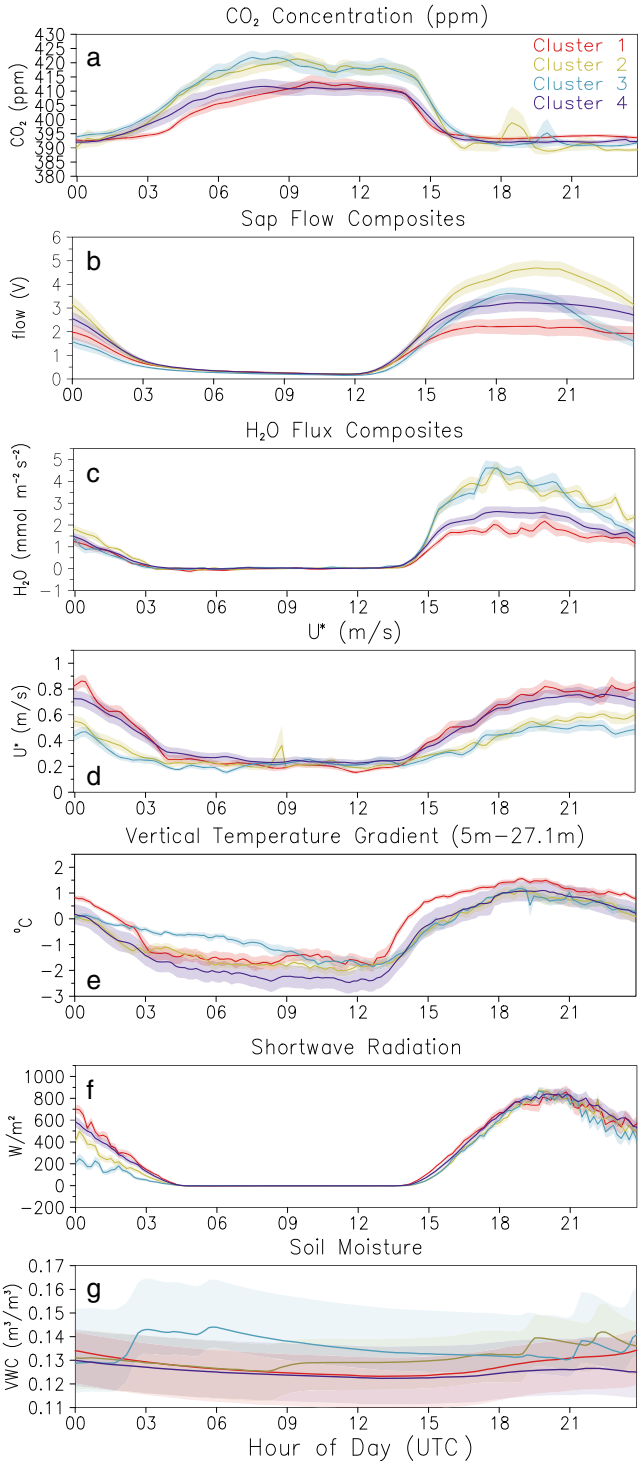


**Figure 8.** Composite diel time series for $CO_2$, Sap Flow, $H_2O$ flux, U* (from the 27.1m sonic anemometer), vertical temperature gradient ($T_{5m}$-$T_{27.1m}$), downward shortwave radiation, and 5 cm soil moisture for the four clusters. The shading shows the standard error for each cluster. Details of the specific instruments used during the campaign can be found in section 2.4.

growing season when summer rain storms were frequent (supporting information Figure 2). This cluster is characterized by a progressive decline in the water vapor mixing ratio that results in a drop of ~4000 ppm at all heights measured (Figures 3d–3f and 4d–4f). These evenings are associated with a decline in $\delta$D and $\delta^{18}$O that is coincident with the changes in specific humidity. The dxs values remain constant amid these other changes. These evenings are characterized by the following: (1) nearly saturated conditions in the canopy as demonstrated by relative humidity (RH) measurements (Figure 5), (2) the highest measurements on the leaf wetness sensors (Figure 7), and (3) a small rise in nighttime surface soil moisture (Figure 8g). These observations suggest this cluster represents the signature of canopy-wide dewfall. The rise in voltage measured from the leaf wetness sensors during dewfall can be related linearly to total water deposition (calculated as the rate of change in water concentration) implying the potential to use these sensors to quantify total moisture deposition (Figure 7), not only as a qualitative indicator of dew or frost as they have been previously utilized [*Griffis et al.*, 2011].

[33] Using the mixing line approach, the $\delta^{18}$O of the dew flux is estimated to vary between 0‰ and 10‰ (Figure 6b). This range encompasses the analytically measured values of collected dew waters (mean of 4.8‰), which provides further support that these nights are indeed dominated by dewfall. Results from the Rayleigh distillation-diffusion box model (supporting information Figure 3) are presented in Figure 9. This model further tests the assumption that the canopy during Cluster 2 evenings is primarily being affected by two processes, dewfall, and diffusion of vapor through the canopy to the site where water is being condensed. The simple model is able to replicate the isotopic vertical profiles in the canopy vapor, suggesting the canopy can be treated principally like a distillation chamber so long as fractionation associated with diffusion is accounted for. We also estimated the isotopic composition of dewfall using equation (3) [*Wen et al.*, 2012] and found values that vary between 5‰ and 10‰. Therefore, in this case, the two models provide comparable skill at predicting the isotopic composition of the dewfall and further support the interpretation that the predominant flux during these evenings is from dew.

### 3.4. Cluster 3: Dewfall in Upper Canopy

[34] Cluster 3 characterizes 18% of the nights and occurs frequently during the early and later portions of the growing season (supporting information Figure 2). This cluster has many of the same characteristics of Cluster 2 in that there is a progressive decline in the water volume mixing ratio of ~4000 ppm with a synchronous drop in isotope ratios and relatively stable dxs values (Figures 3g– 3i and 4g–4i). A significant difference between these two clusters emerges when data from the leaf wetness sensors (Figure 7), soil moisture sensors (Figure 8g), and the vertically resolved mixing line analysis (Figure 6c) are considered. The leaf wetness sensors, which are situated just above the surface, show a moisture peak in the early evening consistent with dewfall. However, the values do not continue to rise through the evening (contrary to Cluster 2), which implies a lack of continued dew accumulation despite the relatively high RH values (Figure 5). Similarly, surface soil moisture shows

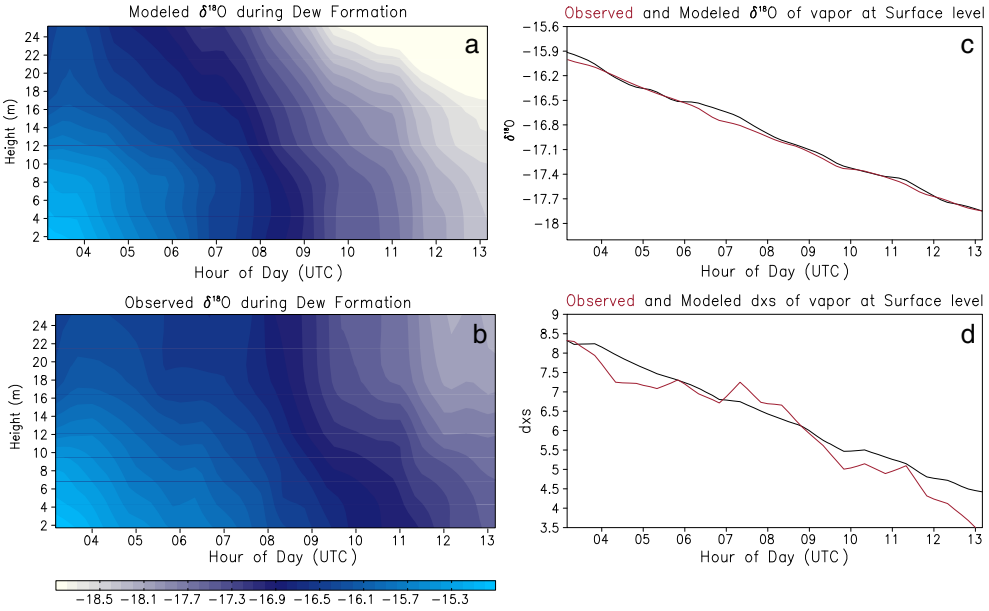


**Figure 9.** (a and black lines in panels c and d) Modeled and (b and red lines in panels c and d) observed isotopic values in the canopy for Cluster 2. The data are only shown for the period during the night when dewfall was occurring. Panels a and b show the isotopic composition of the vapor throughout the canopy from the model (Panel a) and observations (Panel b). Panels c and d show time series of the $\delta^{18}O$ (Panel c) and dxs (Panel d) of the surface vapor. Details of the model are found in section 3.3 and shown schematically in supporting information Figure 1.

a rise in the early evening, which is followed by stability. These two observations imply that surface dewfall only accumulated in the early evening.

[35] The mixing line analysis suggests the fluxes in the upper and lower canopy compartments were disconnected (Figure 6c). The upper canopy is characterized throughout the evening by a flux of ∼10‰ in $\delta^{18}O$, which is similar to what is expected from dewfall while the lower canopy is characterized by fluxes with a similar isotopic ratio as during an average daytime. This cluster therefore captures evenings where dewfall on the surface is only prevalent in the early evening, but dew continues to condense on surfaces of the upper canopy (i.e., leaves) throughout the night. The lower canopy is instead influenced by drainage flows, which yield an isotopic flux similar to above-canopy background values.

### 3.5. Cluster 4: Nighttime Entrainment and Cold Air Drainage

[36] Evenings falling into Cluster 4 are the most common, accounting for close to 50% of the nights. This cluster occurs throughout the growing season without any particularly temporal preference (supporting information Figure 2). From the perspective of water vapor mixing ratios alone, Cluster 4 appears very similar to Cluster 1 in that there is a slight rise in humidity early in the evening followed by a persistently stable period (Figures 3j–3l and 4j–4l). However, $\delta D$, $\delta^{18}O$, and dxs are characterized by relatively constant values during these evenings. We hypothesize that while some exchange between surface liquid and vapor is occurring, the relative isotopic stability during these evenings implies the water cycle is marked primarily by the signature of periodic mixing with above-canopy background vapor. During evenings that are similar to the centroid of Cluster 4, the difference between daytime and nighttime isotopic fluxes in the canopy is about half the magnitude as observed in Cluster 1 (Figure 6d), implying the mixing of above-canopy air is buffering the signature of any within-canopy fluxes that are occurring. This cluster occurs during evenings with the strongest surface winds (Figure 5), highest friction velocities, and the lowest in-canopy $CO_2$ values (Figures 8a and 8d), all of which are indicative of enhanced mixing.

### 3.6. Morning Burst

[37] Each of the aforementioned clusters is associated with a rapid rise in moisture in the morning that is of approximately the same magnitude irrespective of the preceding nocturnal processes (Figures 4a, 4d, 4g, and 4j). A possible technical concern is that this feature could be an artifact of nighttime condensation inside the sample tubing that is released when temperatures rise and RH falls. This concern is ruled out on the basis that a nearby open-path hygrometer shows a comparable feature and that the moisture rise occurs when RH is still at its nighttime maximum and prior to the rapid $CO_2$ and $H_2O$ declines associated with daytime entrainment. The burst in humidity occurs synchronous with the diel rise in sap flow and irradiance (Figure 8) and thus likely represents the signature of morning transpiration, which becomes diluted during the day by entrainment of vapor from above the canopy [*Lai and Ehleringer*, 2011; *Welp et al.*, 2012]. Evidence that this feature is being driven by transpiration is further supported by the observation that the flux occurs first and is most pronounced at the 12 and 17 m inlets, which are closest to the highest density of canopy leaves (see, for example, Figures 3a and 3b).

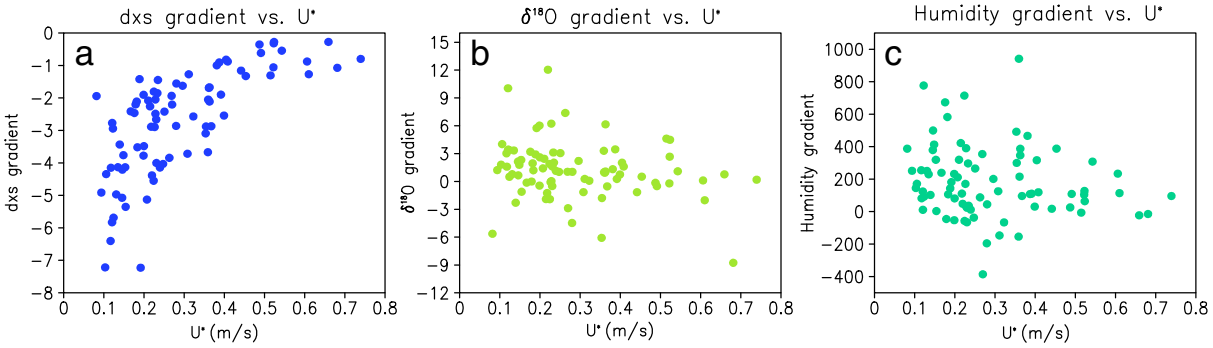


**Figure 10.** The relationship between U* estimated from the measurements at 25.1 m and the vertical gradient in (a) deuterium excess (i.e., $dxs_{25m} - dxs_{12m}$), (b) $\delta^{18}O$, and (c) water volume mixing ratio.

[38] During this transitional period in the morning when turbulence begins to increase, a strong correlation emerges between $U^*$ and the vertical gradient in dxs, which is calculated as the difference between the isotopic values measured at the 12 and 25 m inlets (Figure 10). As particularly well represented during Cluster 1 evenings, the extremely low dxs values of leaf and soil waters place a strong "dxs tag" on within-canopy moisture during the night. This process results in a measurable vertical gradient in dxs that becomes erased in the morning when entrainment acts to flush the canopy. The relationship asymptotes at $U^*$ values greater than 0.5 m/s, which marks the point when the signature of within-canopy processes acting on the moisture, becomes erased by entrainment of air from above the canopy. When similar relationships between $U^*$ and either $\delta^{18}O$ or the mixing ratio of water are sought, no clear correlations emerge (Figure 10). Therefore, dxs appears to provide a uniquely clear tag of moisture influenced by within-canopy processes.

## 4. Discussion

[39] As discussed in previous studies [e.g., *Wright et al.*, 2001; *Friedman et al.*, 2002], seasonal changes in the isotopic composition of moisture in the southwestern U.S. reflect a shift from westerly flow in the fall through spring to surges of monsoonal moisture from the Gulf of California and Gulf of Mexico during the summer months [*Bordoni and Stevens*, 2006; *Bosilovich et al.*, 2003]. The westerly flow that characterizes the winter and spring months brings moisture over significant orographic features en route to Colorado, resulting in moisture that is relatively depleted in heavy isotopes. Moisture during the summer months tends to arrive from the south and east originating from warmer waters and passing over minimal orographic features [*Dominguez et al.*, 2010; *Wright et al.*, 2001]. The isotopic composition of background above-canopy vapor and the daytime fluxes associated with entrainment of this moisture track the seasonal transition in the large-scale circulation patterns (Figure 2).

[40] Unlike the daytime fluxes, which are dominated by entrainment and consequently responsive to the large-scale circulation, the nighttime isotopic dynamics reveal hydrological processes unfolding within the canopy. The nights are separated here into four dominant types using an objective multivariate-clustering algorithm applied to the isotopic and meteorological data. The likelihood that evenings of a given cluster occur varies temporally based on synoptic variability that influences surface wind speed and humidity and lower frequency processes influencing the soil moisture. For example, Cluster 1 (leaf-atmosphere moisture exchange) only occurs during the early season prior to the onset of consistent monsoonal storms while Clusters 2 and 3 (dewfall) are intermingled with one another on synoptic timescales after the onset of the monsoon. It is important to note in consideration of the broader motivation of this study that we find no difference in the EC-derived nighttime water fluxes between the clusters defined here (Figure 8c), yet clearly significant differences in the hydrological processes occur during the evenings that make up the different clusters. Therefore, in terms of quantitatively closing latent heat budgets and understanding how the nocturnal water cycle may influence plant water availability [*Fisher et al.*, 2007], the results presented here, considered alongside other recent laser absorption results from different ecosystems [e.g., *Welp et al.*, 2012; *Wen et al.*, 2008; *Rambo et al.*, 2011], collectively show how this approach can be used to elucidate nocturnal processes.

[41] Dewfall emerged as one of the dominant influences on the nocturnal water cycle (32% of the evenings, Clusters 2 and 3) after the onset of monsoon storms. The presence of dewfall was elicited from the isotopic data using both a Rayleigh distillation model (Figure 9) and through flux analysis using the inverse gradient approach (Figure 6). The presence of dew was confirmed through data from the leaf wetness sensors (Figure 7) and also from informal visual observations of the presence of significant surface water on many of the mornings during the campaign. The frequency of dew events increased significantly following the onset of the monsoon, suggesting that increased surface soil moisture is important to the occurrence of dew. Dewfall was also more likely to occur in specific wind regimes. In their review of the ecological significance of dew, *Stone* [1963] argue that both very strong and very weak winds discourage the formation of dew. Indeed, here we find that dewfall occurred during evenings when winds were slightly below average but not exceedingly still (Figure 5). As mentioned, dewfall was not observed through the EC system and therefore would go unnoticed without additional sensors. The LWS does capture surface dew events and may even be useful to characterize the magnitude of the dew flux (Figure 7), but these sensors miss the events where

dew only fell in the canopy (Cluster 3). According to the analysis here, an approximately equal number of evenings occurred where dew fell in the canopy but not on the surface. This reflects differences in the radiative properties between the soil and leaf surfaces [*Stone*, 1963]. Other techniques for reconstructing dewfall such as through the difference between total evapotranspiration (ET) and precipitation [*Malek et al.*, 1999] could potentially be used, but this technique relies on tight constraints of both ET and precipitation totals and also does not distinguish between foliar and surface dewfall.

[42] The enhanced understanding of dewfall gleaned from isotopes [*Wen et al.*, 2012; *Welp et al.*, 2008] is significant for two primary reasons: (1) dew influences the latent heat budget of the surface and (2) dew may be ecologically significant through foliar absorption or moistening of surface soils [*Stone*, 1963; *Malek et al.*, 1999; *Munné-Bosch et al.*, 1999; *Boucher et al.*, 1995]. Dewfall would generally act to heat the surface of leaves and soil during the evenings and cool the surfaces during the daytime. Dewfall is ultimately a net-zero energy process [*Malek et al.*, 1999], which is to say that the latent heat associated with the condensation of dew must be balanced by the latent heat of evaporation. In this respect, the fact that dewfall is not observed by the EC system would not produce an overall bias in the seasonal energy budget. However, the timescale at which the latent heat of evaporation is compensated by heating from condensation may be significant for balancing the diel energy budget. For example, if condensed dew during the night is immediately released in the morning when RH drops, then the energy is balanced quickly. However, if condensed water acts to moisten mesophyll tissues through foliar uptake [*Munné-Bosch et al.*, 1999; *Munné-Bosch and Alegre*, 1999; *Boucher et al.*, 1995; *Kim and Lee*, 2011] or is adsorbed onto soil with a strong matric potential, the release of this water may significantly lag behind when it is condensed. The timescale of the lag could mean that latent heating from dew condensation may not be fully balanced by evaporative cooling for days or weeks later.

[43] Isotopic flux analysis as done in Figure 6 could theoretically be used to assess the symmetrical nature of dew condensation and subsequent evaporation based on the argument that the isotopic composition of the dew condensate is known and that complete evaporation should yield an isotopically identical flux to the condensate. By examining the isotopic composition of the flux in the morning immediately following the rapid decline in RH (Figure 5), when we assume that most of the dew would be evaporated, we see no clear evidence of a more enriched flux following dewfall rather than nondewfall nights (Figure 6). These observations circumstantially suggest some of the dew that is condensed experiences a lag through adsorption onto the soil surface or through uptake across stomata, which has been shown to occur [*Kim and Lee*, 2011; *Munné-Bosch and Alegre*, 1999]. However, the transpiration flux in the morning is significantly larger than the dew flux and therefore may sufficiently hide the signal associated with dew release. Nonetheless, there is an observed rise in surface soil moisture associated with dewfall that is not reversed during the following day (Figure 8) providing evidence that some percentage of the dew (that adsorbed onto the soil) is not immediately released. A more targeted experiment would be needed to adequately assess the timing that dew water is released. This would likely include more regular isotopic sampling of leaf, shallow soil waters and dew condensate.

[44] While moisture from dew is generally not considered a "limiting factor" for growth in most ecosystems, it is known to be ecologically significant in certain hydrologically stressed regimes [*Malek et al.*, 1999; *Stone*, 1963; *Munné-Bosch et al.*, 1999]. There is now a growing body of literature showing the importance of foliar uptake of both fog waters [*Simonin et al.*, 2009; *Eller et al.*, 2013] and intercepted precipitation [*Breshears et al.*, 2008] as well as results showing the critical role that intercepted fog plays in soil respiration rates [*Carbone et al.*, 2012]. In light of these results, it must be considered likely that frequent dew events would play a role in the terrestrial carbon cycle of forests both through increased assimilation by trees and respiration by soils. Foliar uptake of dew results in a short-term reduction in stomatal conductance [*Munné-Bosch and Alegre*, 1999; *Stone*, 1963] but ultimately leads to a sustained increase in midday stomatal conductance by moistening mesophyll [*Boucher et al.*, 1995; *Munné-Bosch et al.*, 1999]. While the addition of moisture to leaf should theoretically result in a decrease in transpiration rates, the reverse has also been shown where wetting of the cell wall leads to a decrease in the cell wall resistance to evaporation and ultimately an increase in transpiration rates [*Stone*, 1963].

[45] At the MEF site, evenings with measurable dewfall were associated with both the highest overall nighttime $CO_2$ concentrations in the canopy and highest sap flow during the following day (Figure 8). It is possible that these changes could be attributed to the additional liquid water that becomes available from dewfall. However, dewfall is more common during the monsoonal period of the growing season and therefore the enhanced soil and plant fluxes following and during dewfall may simply be circumstantial. Another possibility is the anomalous $CO_2$ concentrations during dewfall nights arose from higher atmospheric stability, which caps the canopy and allows a greater buildup of respired $CO_2$ during the night [*Hollinger et al.*, 1994]. Metrics of stability during the different clusters, including $U^*$ and vertical temperature gradients (Figure 8), do not indicate that dewfall nights were significantly more stable than the other clusters. This is consistent with previous work suggesting dewfall is most common during evenings of intermediate stability [*Stone*, 1963] and indicates a realistic possibility that moisture from dew may increase the respiration flux [*Rustad et al.*, 2000]. This process would be analogous to the way intercepted fog produces an increase in microbial activity in soils [*Carbone et al.*, 2012]. It is also unlikely that dewfall influences sap flow of the trees directly through its effect on soil moisture as the isotopic composition of the stem and leaf waters (Figure 2) indicates these trees are drawing on waters that are significantly more depleted than dew condensate. However, a cursory analysis of the isotopic ratio in waters from grasses and forbs at MEF (not shown) suggests these species are relying on moisture sources that are isotopically enriched (approaching 0‰) and therefore may be able to directly take advantage of the small increase in surface soil moisture associated with dewfall.

[46] The results encourage a number of questions regarding the significance of dewfall from an energy and carbon

budget perspective, which could be pursued using Land Surface Models. An immediate test would be assessing whether model simulations are accurately representing the magnitude and frequency of dew events at sites where isotopic measurements allow some quantitative information on dew fall. If the downward flux of dew is correct, the models would provide a tool to test how the lag between dewfall and dew release influences the energy and carbon budgets of an ecosystem. Depending on the significance that dewfall has on carbon cycling, it could become critical to ask whether changes in regional climates predicted to unfold in the coming decades with the continued rise in atmospheric $CO_2$ concentrations, especially in the semiarid regions like MEF [*Rotenberg and Yakir*, 2011], would yield changes in dew flux and ultimately in the carbon efficiency of these ecosystems.

[47] In the early part of the growing season prior to the onset of monsoonal rains, dewfall was not apparent. During these periods, the stillest evenings showed clear indications of exchange between the canopy air and leaf and soil pools (Cluster 1). The isotopic exchange between the canopy vapor and liquid pools acts to enrich the canopy vapor in heavy isotopes and reduce the dxs value while ultimately not yielding an overall flux of total water to the system (Figures 3a–3c and 4a–4c). The exception occurs during the early part of the evening when skin and air temperatures are offset from one another such that the saturation vapor pressure is different, resulting in a positive flux from surface to canopy following the vapor pressure gradient between leaf and soil boundary air, on the one hand, and the canopy air space on the other. A simple two-box model can be used to test this explanation of Cluster 1, where one box is the leaf/soil boundary vapor and the other is the canopy vapor and the two are approaching equilibrium. We take the leaf water isotopic value to be the average of all measurements (Figure 2e) ($\delta^{18}O$ = 16‰ and $\delta D$ = – 10‰), which yields a vapor that is offset from the liquid by the temperature-dependent fractionation factor (i.e., $\alpha$ from *Majoube* [1971]). The canopy vapor $\delta D$ and $\delta^{18}O$ values are initialized according to the observed values in the beginning of the evening (–170‰ and –22‰) and the two boxes approach full equilibration. In order to accommodate the approximate 3‰ rise in $\delta^{18}O$ and the 14‰ decline in dxs (Figures 4b and 4c), we approximate the vapor must approach 12% of the way towards equilibrium.

[48] We did not observe anomalously high sap flow during these nights so it is not likely that there was significant water loss from the plants; yet there remained persistent exchange between the isotopically enriched and low dxs waters of the plant and soil surface with the canopy moisture. Because surface soil waters are not sufficiently enriched to account for observed isotopic changes in the canopy, we assume the larger source of exchange is occurring across the leaf as opposed to the soil surface. Ultimately, the observed exchange process has only a negligible influence on nighttime moisture and energy budgets but characterizing the signature of this process provides a tool to track when gas exchange across open stomata is occurring.

[49] A useful feature that arises from the exchange process is that moisture in the canopy becomes "tagged" and can therefore be traced as it mixes into the above-canopy air. This is clearly observable by plotting morning vertical gradients in dxs between within (12 m) and above (25.1 m) canopy moisture against $U^*$ (Figure 10). When $U^*$ values are low, there is a strong dxs gradient reflecting the direct impact the canopy is having on the isotopic composition of the canopy moisture relative to the air above. As $U^*$ values increase and the canopy moisture is flushed, the gradient becomes relaxed. When a similar regression is calculated between specific humidity or $\delta^{18}O$ gradients and $U^*$, no such relationship emerges, which show that these are not effective tracers at capturing the mixing of canopy-affected moisture into the open atmosphere. Therefore, because of its greater sensitivity to condensation and evaporation, dxs provides a strong observational constraint on exchange between surface ecosystem waters and the air.

[50] The evenings that fell into Clusters 1–3 were associated with hydrological processes that have potentially significant influences on the water budget of this forest. However, the majority of evenings were overwhelmingly characterized by mixing with above-canopy air, which occurs during nights of relatively low humidities, low $CO_2$ concentrations, and strong surface winds. During these nights, the humidity and isotopic composition of moisture remained nearly constant. This is not to negate the possibility of small contributions from other processes, but the water cycle during the evenings is predominantly inactive and assumptions that nighttime latent heat and fluxes are negligible, as inferred from the EC data, and are likely valid.

## 5. Conclusion

[51] The proliferation of Laser Absorption Spectrometry (LAS) instrumentation is now enabling an efficient means to make high-resolution measurements of ambient isotope species (in both $CO_2$ and $H_2O$) that can be used to assess fluxes in a way that is independent of and complementary to EC techniques. Specifically, when used in conjunction with below-canopy EC measurements, nighttime fluxes can be estimated from the isotope ratios (when there is low turbulence) and daytime fluxes can be estimated with EC when the isotope ratios are overwhelmingly influenced by entrainment. In this study we chose to adopt a novel compositing approach, which highlighted dominant processes of the nighttime water cycle that would have gone undetected using more classical techniques. Despite the loss of some information that arises from compositing, the technique provides a simple method to highlight first-order processes and minimizes the impact of analytical uncertainties associated with accurate calibration of high-frequency in situ isotopic measurements. The study shows the way isotopic measurements can be used to quantify the frequency and magnitude of dew events and highlights that this was a significant component of the water cycle at this midlatitude open-canopy forest site. The results come in light of growing evidence of the importance of foliar absorption for plant water budgets, and we suggest that additional more targeted experiments would be useful to assess the significance that dew plays in the carbon and energy budgets of forests. In addition, we show that isotopic measurements, particularly the second-order *deuterium excess* parameter, are a sensitive tracer of exchange between canopy vapor and leaf waters. This is useful in considering that emissions from forests have a significant influence on the chemical composition of air masses and ultimately in mediating precipitation

[*Spracklen et al.*, 2012]. With the imminent launching of the National Ecological Observatory Network, which will provide 20 sites in the U.S. that will continuously monitor the isotopic composition of water vapor, the ability to use isotope ratio information as a complement to flux data toward understanding the water cycle during stable periods will have important implications in understanding water usage by plants and closing forest energy budgets.

[52] **Acknowledgments.** The authors would like to thank Mariel Herzog and Francina Dominguez for assistance with the liquid analysis, Peter Harley and Russ Monson for assistance with the MEF facilities and field support. C.J.S. acknowledges the support of a CIRES Visiting Faculty Fellowship. M.B., A.B., and D.N. were supported by the National Science Foundation Climate and Large Scale Dynamics program as part of an Faculty Early Career Development award (AGS-0955841). Support for David Gochis and Andrew Turnipseed was provided by the National Science Foundation through its support of NCAR and for NCAR technical staff through NSF grant EAR-0910831. The reported research was partially supported by Los Alamos National Laboratory Directed Research and Development Project entitled Isotopic Tracer for Climate Relevant Secondary Organic Aerosol (20090425ER).

## References

Adams, H., M. Guardiola-Claramonte, G. Barron-Gafford, J. Villegas, D. Breshears, C. Zou, P. Troch, and T. Huxman (2009), Temperature sensitivity of drought-induced tree mortality portends increased regional die-off under global change-type drought, *Proc. Natl. Acad. Sci.*, *106*(17), 7063–7066.

Allison, G., J. Gat, and F. Leaney (1985), The relationship between deuterium and oxygen-18 delta values in leaf water, *Chem. Geol. Isot. Geosci. Sect.*, *58*(1), 145–156.

Allison, G. B., and C. J. Barnes (1983), Estimation of evaporation from non-vegetated surfaces using natural deuterium, *Nature*, *301*(5896), 143–145.

Anthoni, P., M. Unsworth, B. Law, J. Irvine, D. Baldocchi, S. Tuyl, and D. Moore (2002), Seasonal differences in carbon and water vapor exchange in young and old-growth ponderosa pine ecosystems, *Agric. For. Meteorol.*, *111*(3), 203–222.

Bala, G., K. Caldeira, M. Wickett, T. Phillips, D. Lobell, C. Delire, and A. Mirin (2007), Combined climate and carbon-cycle effects of large-scale deforestation, *Proc. Natl. Acad. Sci.*, *104*(16), 6550–6555.

Baldocchi, D., et al. (2001), FLUXNET: A new tool to study the temporal and spatial variability of ecosystem-scale carbon dioxide, water vapor, and energy flux densities, *Bull. Am. Meteorol. Soc.*, *82*(11), 2415–2434.

Beer, C., et al. (2010), Terrestrial gross carbon dioxide uptake: Global distribution and covariation with climate, *Science*, *329*(5993), 834–838.

Blumen, W. (1984), An observational study of instability and turbulence in nighttime drainage winds, *Boundary Layer Meteorol.*, *28*(3), 245–269.

Bordoni, S., and B. Stevens (2006), Principal component analysis of the summertime winds over the Gulf of California: A gulf surge index, *Mon. Weather Rev.*, *134*(11), 3395–3414.

Bosilovich, M., Y. Sud, S. Schubert, and G. Walker (2003), Numerical simulation of the large-scale North American monsoon water sources, *J. Geophys. Res.*, *108*(D16), 8614, doi:10.1029/2002JD003095.

Boucher, J.-F., A. Munson, and P. Bernier (1995), Foliar absorption of dew influences shoot water potential and root growth in Pinus strobus seedlings, *Tree Physiol.*, *15*(12), 819–823.

Breshears, D. D., N. G. McDowell, K. L. Goddard, K. E. Dayem, S. N. Martens, C. W. Meyer, and K. M. Brown (2008), Foliar absorption of intercepted rainfall improves woody plant water status most during drought, *Ecology*, *89*(1), 41–47.

Brooks, J., H. Barnard, R. Coulombe, and J. McDonnell (2010), Ecohydrologic separation of water between trees and streams in a Mediterranean climate, *Nat. Geosci.*, *3*(2), 100–104.

Burgess, S., M. Adams, N. Turner, C. Beverly, C. Ong, A. Khan, and T. Bleby (2001), An improved heat pulse method to measure low and reverse rates of sap flow in woody plants, *Tree Physiol.*, *21*(9), 589–598.

Calder, I. (1998), Water use by forests, limits and controls, *Tree Physiol.*, *18*(8–9), 625–631.

Caldwell, M., T. Dawson, and J. Richards (1998), Hydraulic lift: Consequences of water efflux from the roots of plants, *Oecologia*, *113*(2), 151–161.

Carbone, M., A. Williams, A. Ambrose, C. Boot, E. Bradley, T. Dawson, S. Schaeffer, J. Schimel, and C. Still (2012), Cloud shading and fog drip influence the metabolism of a coastal pine ecosystem, *Global Change Biol.*, *19*(2), 484–497.

Craig, H., and L. Gordon (1965), Deuterium and $^{18}O$ variations in the ocean and the marine atmosphere, *Stable Isotopes in Oceanographic Studies and Paleotemperatures, Spoleto*, *9*, 1–122.

Dansgaard, W. (1964), Stable isotopes in precipitation, *Tellus*, *16*, 436–468.

Dawson, T. (1998), Fog in the California redwood forest: Ecosystem inputs and use by plants, *Oecologia*, *117*(4), 476–485.

Dawson, T. E., and J. R. Ehleringer (1991), Streamside trees that do not use stream water, *Nature*, *350*(6316), 335–337.

de Roode, S., F. Bosveld, and P. Kroon (2010), Dew formation, eddy-correlation latent heat fluxes, and the surface energy imbalance at Cabauw during stable conditions, *Boundary Layer Meteorol.*, *135*(3), 369–383.

DiGangi, J., et al. (2011), First direct measurements of formaldehyde flux via eddy covariance: Implications for missing in-canopy formaldehyde sources, *Atmos. Chem. Phys.*, *11*, 10,565–10,578.

DiGangi, J., et al. (2012), Observations of glyoxal and formaldehyde as metrics for the anthropogenic impact on rural photochemistry, *Atmos. Chem. Phys. Discuss.*, *12*, 6049–6084.

Dominguez, F., D. Gochis, P. Harley, A. Turnipseed, and J. Hu (2010), Transpiration and evaporation measurements in a mountain ecosystem using real-time field-based water vapor isotopes, in *EOS Transactions. AGU*, pp. U33B–05., vol. Fall Meeting Suppl.

Eller, C. B., A. L. Lima, and R. S. Oliveira (2013), Foliar uptake of fog water and transport below ground alleviates drought effects in the cloud forest tree species, Drimys brasiliensis (Winteraceae), *New Phytol.*, *199*(1), 151–62.

Farquhar, G., and K. Gan (2003), On the progressive enrichment of the oxygen isotopic composition of water along a leaf, *Plant Cell Env.*, *26*(9), 1579–1597.

Fisher, J., D. Baldocchi, L. Misson, T. Dawson, and A. Goldstein (2007), What the towers don't see at night: Nocturnal sap flow in trees and shrubs at two AmeriFlux sites in California, *Tree Physiol.*, *27*(4), 597–610.

Flanagan, L., J. Ehleringer, and J. Marshall (1992), Differential uptake of summer precipitation among co-occurring trees and shrubs in a pinyon-juniper woodland, *Plant Cell Env.*, *15*(7), 831–836.

Friedman, I., G. I. Smith, J. D. Gleason, A. Warden, and J. M. Harris (1992), Stable isotope composition of waters in Southeastern California. 1. Modern precipitation, *J. Geophys. Res.*, *97*(D5), 5795–5812, doi:10.1029/92JD00184.

Friedman, I., J. M. Harris, G. I. Smith, and C. A. Johnson (2002), Stable isotope composition of waters in the Great Basin, United States. 1. Air-mass trajectories, *J. Geophys. Res.*, *107*(19), 1–14, doi:10.1029/92JD00184.

Griffis, T., J. Zhang, J. Baker, N. Kljun, and K. Billmark (2007), Determining carbon isotope signatures from micrometeorological measurements: Implications for studying biosphere–atmosphere exchange processes, *Boundary Layer Meteorol.*, *123*(2), 295–316.

Griffis, T., et al. (2010), Determining the oxygen isotope composition of evapotranspiration using eddy covariance, *Boundary Layer Meteorol.*, *137*(2), 307–326.

Griffis, T., X. Lee, J. Baker, K. Billmark, N. Schultz, M. Erickson, X. Zhang, J. Fassbinder, W. Xiao, and N. Hu (2011), Oxygen isotope composition of evapotranspiration and its relation to C4 photosynthetic discrimination, *J. Geophys. Res.*, *116*, G01035, doi:10.1029/2010JG001514.

Gross, G. (1987), Some effects of deforestation on nocturnal drainage flow and local climate — A numerical study, *Boundary Layer Meteorol.*, *38*(4), 315–337.

Gupta, P., D. Noone, J. Galewsky, C. Sweeney, and B. Vaughn (2009), Demonstration of high-precision continuous measurements of water vapor isotopologues in laboratory and remote field deployments using wavelength-scanned cavity ring-down spectroscopy (WS-CRDS) technology, *Rapid. Commun. Mass Spectrom.*, *23*(16), 2534–2542.

Helliker, B. R., J. S. Roden, C. Cook, and J. R. Ehleringer (2002), A rapid and precise method for sampling and determining the oxygen isotope ratio of atmospheric water vapor, *Rapid Commun. Mass Spectrom.*, *16*(10), 929–932.

Hollinger, D., F. Kelliher, J. Byers, J. Hunt, T. McSeveny, and P. Weir (1994), Carbon dioxide exchange between an undisturbed old-growth temperate forest and the atmosphere, *Ecology*, 134–150.

Horita, J., and D. Wesolowski (1994), Liquid-vapor fractionation of oxygen and hydrogen isotopes of water from the freezing to the critical temperature, *Geochim. Cosmochim. Acta*, *58*(16), 3425–3437.

Jacobs, A., B. Heusinkveld, R. W. Kruit, and S. Berkowicz (2006), Contribution of dew to the water budget of a grassland area in the Netherlands, *Water Resour. Res.*, *42*, W03415, doi:10.1029/2005WR004055.

Johnson, W. (1956), The effect of grazing intensity on plant composition, vigor, and growth of pine-bunchgrass ranges in central Colorado, *Ecology*, *37*(4), 790–798.

Kaser, L., (2013), Undisturbed and disturbed above canopy ponderosa pine emissions: PTR-TOF-MS measurements and MEGAN 2.1 model results, *Atmos. Chem. Phys. Discuss.*, *13*, 15,333–15,375.

Keeling, C. (1958), The concentration and isotopic abundances of atmospheric carbon dioxide in rural areas, *Geochim. Cosmochim. Acta*, *13*(4), 322–334.

Keeling, C. (1960), The concentration and isotopic abundances of carbon dioxide in the atmosphere, *Tellus*, *12*(2), 200–203.

Kim, K., and X. Lee (2011), Transition of stable isotope ratios of leaf water under simulated dew formation, *Plant Cell Env.*, *34*(10), 1790–1801.

Kim, S., T. Karl, A. Guenther, G. Tyndall, J. Orlando, P. Harley, R. Rasmussen, and E. Apel (2010), Emissions and ambient distributions of Biogenic Volatile Organic Compounds (BVOC) in a ponderosa pine ecosystem: Interpretation of PTR-MS mass spectra, *Atmos. Chem. Phys.*, *10*(4), 1759–1771.

Lai, C., and J. Ehleringer (2011), Deuterium excess reveals diurnal sources of water vapor in forest air, *Oecologia*, *165*(1), 213–223.

Lai, C., J. Ehleringer, B. Bond, and U. Paw (2006), Contributions of evaporation, isotopic non-steady state transpiration and atmospheric mixing on the $\delta^{18}O$ of water vapour in Pacific Northwest coniferous forests, *Plant Cell Env.*, *29*(1), 77–94.

Lawrence, P., and T. Chase (2009), Climate impacts of making evapotranspiration in the Community Land Model (CLM3) consistent with the Simple Biosphere Model (SiB), *J. Hydrometeorol.*, *10*(2), 374–394.

Lee, J. H., X. H. Feng, E. S. Posmentier, A. M. Faiia, and S. Taylor (2009), Stable isotopic exchange rate constant between snow and liquid water, *Chem. Geol.*, *260*(1-2), 57–62.

Lee, X., J. Huang, and E. Patton (2011), A large-eddy simulation study of water vapour and carbon dioxide isotopes in the atmospheric boundary layer, *Boundary Layer Meteorol.*, 1–20.

Lis, G., L. Wassenaar, and M. Hendry (2008), High-precision laser spectroscopy D/H and $^{18}O/^{16}O$ measurements of microliter natural water samples, *Anal. Chem.*, *80*(1), 287–293.

Loescher, H., B. Law, L. Mahrt, D. Hollinger, J. Campbell, and S. Wofsy (2006), Uncertainties in, and interpretation of, carbon flux estimates using the eddy covariance technique, *J. Geophys. Res.*, *111*, D21S90, doi:10.1029/2005JD006932.

Luyssaert, S., et al. (2007), $CO_2$ balance of boreal, temperate, and tropical forests derived from a global database, *Global Change Biol.*, *13*(12), 2509–2537.

Majoube, M. (1971), Oxygen-18 and deuterium fractionation between water and steam, *J. Chim. Phys. Phys.- Chim. Biol.*, *68*(10), 1423–1436.

Malek, E., G. McCurdy, and B. Giles (1999), Dew contribution to the annual water balances in semi-arid desert valleys, *J. Arid. Environ.*, *42*(2), 71–80.

Massman, W., and X. Lee (2002), Eddy covariance flux corrections and uncertainties in long-term studies of carbon and energy exchanges, *Agric. For. Meteorol.*, *113*(1–4), 121–144.

Massman, W., J. Frank, and N. Reisch (2008), Long-term impacts of prescribed burns on soil thermal conductivity and soil heating at a Colorado Rocky Mountain site: A data/model fusion study, *Int. J. Wildland Fire*, *17*(1), 131–146.

Meinzer, F., J. Brooks, J. Domec, B. Gartner, J. Warren, D. Woodruff, K. Bible, and D. Shaw (2005), Dynamics of water transport and storage in conifers studied with deuterium and heat tracing techniques, *Plant Cell Env.*, *29*(1), 105–114.

Merlivat, L., and J. Jouzel (1979), Global climatic interpretation of the deuterium-oxygen 18 relationship for precipitation, *J. Geophys. Res.*, *84*, 5029–5033, doi:10.1029/JC084iC08p05029.

Miller, J., and P. Tans (2003), Calculating isotopic fractionation from atmospheric measurements at various scales, *Tellus B*, *55*(2), 207–214.

Munné-Bosch, S., and L. Alegre (1999), Role of dew on the recovery of water-stressed Melissa officinalis plants, *J. Plant Physiol.*, *154*(5), 759–766.

Munné-Bosch, S., S. Nogués, and L. Alegre (1999), Diurnal variations of photosynthesis and dew absorption by leaves in two evergreen shrubs growing in Mediterranean field conditions, *New Phytol.*, *144*(1), 109–119.

Myneni, R., J. Dong, C. Tucker, R. Kaufmann, P. Kauppi, J. Liski, L. Zhou, V. Alexeyev, and M. Hughes (2001), A large carbon sink in the woody biomass of northern forests, *Proc. Natl. Acad. Sci.*, *98*(26), 14,784–14,789.

Nippert, J. B., J. J. Butler Jr, G. J. Kluitenberg, D. O. Whittemore, D. Arnold, S. E. Spal, and J. K. Ward (2010), Patterns of Tamarix water use during a record drought, *Oecologia*, *162*(2), 283–292.

Noone, D., et al. (2013), Determining water sources in the boundary layer from tall tower profiles of water vapor and surface water isotope ratios after a snowstorm in Colorado, *Atmos. Chem. Phys.*, *13*, 1607–1623.

Pataki, D., J. Ehleringer, L. Flanagan, D. Yakir, D. Bowling, C. Still, N. Buchmann, J. Kaplan, and J. Berry (2003), The application and interpretation of Keeling plots in terrestrial carbon cycle research, *Global Biogeochem. Cycles*, *17*(1), 1022, doi:10.1029/2001GB001850.

Pitman, A., et al. (2009), Uncertainties in climate responses to past land cover change: First results from the LUCID intercomparison study, *Geophys. Res. Lett.*, *36*, L14814, doi:10.1029/2009GL039076.

Rambo, J., C. Lai, J. Farlin, M. Schroeder, and K. Bible (2011), On-site calibration for high precision measurements of water vapor isotope ratios using off-axis cavity-enhanced absorption spectroscopy, *J. Atmos. Oceanic Technol.*, *28*, 1448–1457.

Rotenberg, E., and D. Yakir (2011), Distinct patterns of changes in surface energy budget associated with forestation in the semiarid region, *Global Change Biol.*, *17*(4), 1536–1548.

Rustad, L., T. Huntington, and R. Boone (2000), Controls on soil respiration: Implications for climate change, *Biogeochemistry*, *48*(1), 1–6.

Schmidt, M., K. Maseyk, C. Lett, P. Biron, P. Richard, T. Bariac, and U. Seibt (2012), Reducing and correcting for contamination of ecosystem water stable isotopes measured by isotope ratio infrared spectroscopy, *Rapid Commun. Mass Spectrom.*, *26*(2), 141–153.

Schultz, N., T. Griffis, X. Lee, and J. Baker (2011), Identification and correction of spectral contamination in $^{2}H/^{1}H$ and $^{18}O/^{16}O$ measured in leaf, stem, and soil water, *Rapid Commun. Mass Spectrom.*, *25*(21), 3360–3368.

Schuster, J. (1964), Root development of native plants under three grazing intensities, *Ecology*, *45*(1), 63–70.

Shu, Y., X. H. Feng, E. S. Posmentier, L. J. Sonder, A. M. Faiia, and D. Yakir (2008), Isotopic studies of leaf water. Part 1: A physically based two-dimensional model for pine needles, *Geochim. Cosmochim. Acta*, *72*(21), 5175–5188.

Simonin, K. A., L. S. Santiago, and T. E. Dawson (2009), Fog interception by Sequoia sempervirens (D. Don) crowns decouples physiology from soil water deficit, *Plant Cell Env.*, *32*(7), 882–892.

Spracklen, D., S. Arnold, and C. Taylor (2012), Observations of increased tropical rainfall preceded by air passage over forests, *Nature*, *489*, 282–285.

Steen-Larsen, H., et al. (2013), Continuous monitoring of summer surface water vapor isotopic composition above the Greenland Ice Sheet, *Atmos. Chem. Phys.*, *13*(9), 4815–4828.

Stewart, J., and A. Thom (1973), Energy budgets in pine forest, *Q. J. R. Meteorol. Soc.*, *99*(419), 154–170.

Still, C., J. Berry, M. Ribas-Carbo, and B. Helliker (2003), The contribution of C3 and C4 plants to the carbon cycle of a tallgrass prairie: An isotopic approach, *Oecologia*, *136*(3), 347–359.

Still, C., et al. (2009), The influence of clouds and diffuse radiation on ecosystem-atmosphere $CO_2$ and $CO^{18}O$ exchanges, *J. Geophys. Res.*, *114*, G01018, doi:10.1029/2007JG000675.

Stone, E. C. (1963), The ecological importance of dew, *Q. Rev. Biol.*, 328–341.

Strong, M. (2012), Variations in the stable isotope compositions of water vapor and precipitation in New Mexico: Links to synoptic-scale weather, Ph.D. thesis, The University of New Mexico.

Stull, R. (1988), *An Introduction To Boundary Layer Meteorology*, pp. 10–30, vol. 13, Springer, Dordrecht, The Netherlands.

Tremoy, G., F. Vimeux, O. Cattani, S. Mayaki, I. Souley, and G. Favreau (2011), Measurements of water vapor isotope ratios with wavelength-scanned cavity ring-down spectroscopy technology: New insights and important caveats for deuterium excess measurements in tropical areas in comparison with isotope-ratio mass spectrometry, *Rapid Commun. Mass Spectrom.*, *25*(23), 3469–3480.

Vickers, D., J. Irvine, J. Martin, and B. Law (2012), Nocturnal subcanopy flow regimes and missing carbon dioxide, *Agric. For. Meteorol.*, *152*, 101–108.

Wang, L., K. Caylor, J. Villegas, G. Barron-Gafford, D. Breshears, and T. Huxman (2010), Partitioning evapotranspiration across gradients of woody plant cover: Assessment of a stable isotope technique, *Geophys. Res. Lett.*, *37*, L09401, doi:10.1029/2010GL043228.

Welp, L., X. Lee, K. Kim, T. Griffis, K. Billmark, and J. Baker (2008), $\delta^{18}O$ of water vapour, evapotranspiration and the sites of leaf water evaporation in a soybean canopy, *Plant Cell Env.*, *31*(9), 1214–1228.

Welp, L., X. Lee, T. Griffis, X. Wen, S. Li, X. Sun, Z. Hu, M. Martin, and J. Huang (2012), A meta-analysis of water vapor deuterium-excess in the midlatitude atmospheric surface layer, *Global Biogeochem. Cycles*, *26*, doi:10.1029/2011GB004246.

Wen, X., X. Sun, S. Zhang, G. Yu, S. Sargent, and X. Lee (2008), Continuous measurement of water vapor D/H and 18O/16O isotope ratios in the atmosphere, *J. Hydrol.*, *349*(3-4), 489–500.

Wen, X., X. Lee, X. Sun, J. Wang, Z. Hu, S. Li, and G. Yu (2012), Dew water isotopic ratios and their relationships to ecosystem water pools

and fluxes in a cropland and a grassland in China, *Oecologia*, *168*(2), 549–561.

West, A., S. Patrickson, and J. Ehleringer (2006), Water extraction times for plant and soil materials used in stable isotope analysis, *Rapid Commun. Mass Spectrom.*, *20*(8), 1317–1321.

West, A., G. Goldsmith, P. Brooks, and T. Dawson (2010), Discrepancies between isotope ratio infrared spectroscopy and isotope ratio mass spectrometry for the stable isotope analysis of plant and soil waters, *Rapid Commun. Mass Spectrom.*, *24*(14), 1948–1954.

Williams, A., C. Still, D. Fischer, and S. Leavitt (2008), The influence of summertime fog and overcast clouds on the growth of a coastal Californian pine: A tree-ring study, *Oecologia*, *156*(3), 601–611.

Williams, D., et al. (2004), Evapotranspiration components determined by stable isotope, sap flow and eddy covariance techniques, *Agric. For. Meteorol.*, *125*(3), 241–258.

Wright, W. E., A. Long, A. C. Comrie, S. W. Leavitt, T. Cavazos, and C. Eastoe (2001), Monsoonal moisture sources revealed using temperature, precipitation, and precipitation stable isotope timeseries, *Geophys. Res. Lett.*, *28*(5), 787–790, doi:10.1029/2000GL012094.

Yakir, D., and L. Sternberg (2000), The use of stable isotopes to study ecosystem gas exchange, *Oecologia*, *123*(3), 297–311.

Yepez, E., D. Williams, R. Scott, and G. Lin (2003), Partitioning overstory and understory evapotranspiration in a semiarid savanna woodland from the isotopic composition of water vapor, *Agric. For. Meteorol.*, *119*(1-2), 53–68.

Zimmermann, U., D. Ehhalt, and K. Munnich (1967), Soil-water movement and evapotranspiration: Changes in the isotopic composition of the water, *Isot. Hydrol Vien. Int. Atom. Energy Agency*, 567–585.